REPORT DOCUMENTATION PAGE

AFRL-SR-AR-TR-04-

0026

1. REPORT DATE *(DD-MM-YYYY)*	2. REPORT TYPE	3. DATES COVERED *(From - To)*
	Final Report	Feb 1, 01 - Jun 30, 03

4. TITLE AND SUBTITLE
Neutral Density structures in the High Latitude Thermosphere

5a. CONTRACT NUMBER

5b. GRANT NUMBER
F49620-01-1-0059

5c. PROGRAM ELEMENT NUMBER

6. AUTHOR(S)
Dr. Geoffrey Crowley

5d. PROJECT NUMBER

5e. TASK NUMBER

5f. WORK UNIT NUMBER

7. PERFORMING ORGANIZATION NAME(S) AND ADDRESS(ES)
Southwest Research Institute
6220 Culebra Rd. (78238-5166)
P. O. Drawer 28510 (78228-0510)
Building 178
San Antonio, TX

8. PERFORMING ORGANIZATION REPORT NUMBER

9. SPONSORING/MONITORING AGENCY NAME(S) AND ADDRESS(ES)
Department of the Air Force
Air Force Office of Scientific Research
4015 Wilson Blvd.
Arlington, VA 22203-1954

10. SPONSOR/MONITOR'S ACRONYM(S)

11. SPONSOR/MONITOR'S REPORT NUMBER(S)

12. DISTRIBUTION/AVAILABILITY STATEMENT

Distribution Statement A: Approved for public release. Distribution unlimited

13. SUPPLEMENTARY NOTES
DODAAD CODE: 26401
AFOSR Program Manager: Major Paul Bellaire

20040130 060

14. ABSTRACT

The proposed work will involve the use of a global 3-D first-principles model of the upper atmosphere called the Thermosphere Ionosphere Mesosphere Electrodynamics General Circulation Model (TIMEGCM). The main data sources will be FUV images from the Dynamics Explorer-I (DE-1) satellite, together with in-situ data from the DE-2 satellite. The main focus of this proposal is to investigate whether high latitude neutral density cells can be detected by the advanced ultraviolet remote sensing experiments to be flown on DoD satellites in the near future, such as the Special Sensor Ultraviolet Spectrographic Imager (SSUSI).

15. SUBJECT TERMS

16. SECURITY CLASSIFICATION OF:			17. LIMITATION OF ABSTRACT	18. NUMBER OF PAGES	19a. NAME OF RESPONSIBLE PERSON
a. REPORT	b. ABSTRACT	c. THIS PAGE			Dr. Jeffrey Crowley
					19b. TELEPHONE NUMBER *(Include area code)*

Final Report for Award # F496200110059P00001

PI: Dr. Geoff Crowley

Title: Neutral Density Structures in the High Latitude Thermosphere

Effective Date: April 10, 2001

Report Due: September 1st, 2003

Institution: **Southwest Research Institute**
6220 Culebra Road
San Antonio, TX 78238-5166

1. STATEMENT OF OBJECTIVES

Orbit-averaged density can be predicted to within 5% uncertainty by empirical models using a recently-developed calibration scheme based on an accurate knowledge of a 'test-satellite' orbit. Despite this technique, at high latitudes the empirical models may be in error by a factor of 100% because of their inability to specify the high latitude neutral density 'cells'. The goal of the work proposed here is to develop the use of FUV observations of polar cap composition variations to specify the neutral density cell locations and magnitudes. This information could then be used to correct the empirical models and to reduce the uncertainty in the high latitude density.

The proposed work will involve the use of a global 3-D first-principles model of the upper atmosphere called the Thermosphere Ionosphere Mesosphere Electrodynamics General Circulation Model (TIMEGCM). The main data sources will be FUV images from the Dynamics Explorer-1 (DE-1) satellite, together with in-situ data from the DE-2 satellite. The main focus of this proposal is to investigate whether high latitude neutral density cells can be detected by the advanced ultraviolet remote sensing experiments to be flown on DoD satellites in the near future, such as the Special Sensor Ultraviolet Spectrographic Imager (SSUSI).

The following objectives were addressed in the proposal:

1) Determine what are the composition variations corresponding to the density variations in the high latitude density cells.

The TIMEGCM will be used to perform 24 numerical experiments to explore the response of the thermospheric composition in the density cells for different magnetic activity levels, seasons and IMF By configurations.

2) Determine what are the likely UV signatures of these composition variations.

The brightness of the FUV dayglow is directly related to the ratio of the column integrated concentrations of O and N_2 ($[O]/[N_2]$) in the thermosphere. Therefore the column integrated O/N2 ratio is the key parameter to determine whether the high latitude density cells and the corresponding composition variations will be detectable in the FUV. The likely FUV signatures of the composition variations in the density cells will be determined from the simulations in the 24 numerical experiments.

3) Determine whether there is any evidence of the density (or composition) cells in existing UV images, such as those from the DE-1 satellite.

At this point we turn to the DE-1 images themselves and search for likely signatures. Our search will begin with the February 1983 time frame, which we have already simulated using the TIMEGCM. An initial comparison of the high latitude column integrated O/N2 ratio from the model versus two DE-1 images from that period indicate clear polar cap brightness reductions in the DE-1 images and ($[O]/[N_2]$) depletions in the model. This analysis will indicate whether the density cells could be detected by the SSUSI UV remote sensing instrument to be flown on DMSP satellites within the next year.

4) Investigate whether there is a firm relationship between the UV signatures caused by composition variations and the corresponding neutral density variations that would affect satellite drag.

For this task, the TIMEGCM model and the DE-2 in-situ data will complement the DE-1 images. The most pressing questions are:

(1) How do the location and horizontal extent of the modeled O/N2 depletion relate to the location and horizontal extent of the underlying density cells?

(2) How does the magnitude of the O/N2 depletion relate to the magnitude of the density cell structure?

The proposed research is expected to disclose firm relationships between these quantities. Closure will be achieved by testing these relationships using data from the DE-1 and DE-2 satellites.

5) Explore how knowledge of the existence, location and magnitude of density cells could be incorporated into existing Air Force density prediction procedures for the high latitude regions. Another form of closure will be achieved by exploring ways to use the above relationships operationally with SSUSI data from DMSP. If we are able to specify the location, extent and magnitude of the neutral density cells, as proposed here, we anticipate being able to significantly reduce the high latitude uncertainty in the operational models. An uncertainty of 25% or less seems like a reasonable objective.

2. STATUS OF EFFORT

The work was funded for a total of $80K. The project has been completed successfully, and all funds expended. We have obtained several new results during this work. Some have already been published and others will be publishable in the near future. We were not able to fully complete the proposed tasks for the funded amount, but we have made enough progress to show that the proposed idea of using FUV images to identify density cells is potentially useful for the Air Force mission.

3. SUMMARY OF ACCOMPLISHMENTS BY TASK

- ***Task 1***
  - we have shown for the first time what is the compositional structure underlying the high latitude thermospheric density cells
  - we have shown for the first time that both the cell structures and the underlying composition variations are rotated by changes in the Interplanetary Magnetic Field (IMF) By-component.
- ***Task 2***
  - we have demonstrated the likely UV signatures of the composition variations
  - we showed that they produce effects that are observable by FUV imagers.
- ***Task 3***
  - (Task 3) we have examined DE-2 *in-situ* measurements of composition, together with simultaneous FUV dayglow images from the DE-1 satellite. The DE-1 images were provided by Dr. Tom Immel (U.C. Berkeley).

➢ ***Task 4***

- our simulations showed that there will be a relationship between features in the FUV images, and cellular structures in the neutral density that affect satellite orbits.
- more work is required to obtain a quantitative relationship between the density cells and the O/N2 depletions observed by FUV imagers. In particular, we showed from simulations that the relationship depends on altitude, and we were only able to quantify the relationship at lower altitudes in this effort.
- we found copious evidence of density cells in the in-situ data, but it was not possible to unambiguously correlate this structure with features in the DE-1 FUV images. More work would be required to perform a more detailed study. The best candidates are the December 1982 and Jan-Feb 1983 period, when DE-2 obtained good images of the southern high latitudes, and DE-1 was in a relatively low altitude (250-350 km) orbit that was beginning to circularize.
- we developed a simple correction for the DE-2 data to account for the altitude variation of the satellite during its elliptical orbit. This makes it easier to identify significant density perturbations, because the exponential changes introduced by the altitude variation have been removed.

➢ ***Task 5***

- we serve on the DMSP neutral density and dayside ionosphere Cal-Val teams for the UV sensors launched in the Fall of 2003.
- We have become registered users of the Air Force High Accuracy Satellite Drag Model (HASDM) and have been providing TIMEGCM simulation results for comparison with HASDM, and for density studies. We have discussed the possibility of using UV images to help improve HASDM.

4. COMPREHENSIVE TECHNICAL SUMMARY OF SIGNIFICANT WORK

4.1. INTRODUCTION

Why is density and composition important?

The US Strategic Command (USSTRATCOM) tracks about 8,500 man-made space objects orbiting Earth that are 10 centimeters or larger. These space objects consist of active/inactive satellites, spent rocket bodies, or fragmentation. About 7 percent are operational satellites, 15 percent are rocket bodies, and about 78 percent are fragmentation and inactive satellites. For the next few years, worldwide, about 120 new satellites per year are conservatively expected to be launched, and this number will multiply if the dream of nano-satellite fleets ever becomes reality.

A major reason for tracking orbiting objects is for manned space flight safety and the protection of space assets. For example, as of January 2003, the International Space Station had been reoriented six times to avoid collisions with orbiting debris. During shuttle missions, USSTRATCOM computes possible close approaches of other orbiting objects with the shuttle's flight path. NASA is also advised of space objects that come within a safety box that measures 10 by 10 by 50 kilometers of the orbiter, and it is not uncommon for the Shuttle to maneuver to avoid predicted conjunctions with space debris.

Changes in the density and composition of the neutral atmosphere create variable satellite drag, adversely affecting missions involving space assets, such as collision avoidance. Atmospheric drag is the dominant error source in force models used to predict low perigee (<600 km) satellite trajectories. Predicting the orbits of the shuttle, space station and the debris field in LEO requires accurate (to better than 5%) specification of neutral densities for use in Special Perturbation orbit prediction operations. The current capability of empirical models is an orbit-averaged standard deviation of ~15%-30% (Liu et al., 1983; Marcos 1990). The assimilation of orbital information from dozens of satellites to estimate the global density field using the High Accuracy Satellite Drag Model (HASDM) has recently demonstrated that this can be improved to 5% in the 300-500 km altitude range (Storz et al., 2002; Casali and Barker, 2002; Wise et al., 2002). The HASDM program employed 60-75 calibration satellites to real-time correct an empirical model atmosphere over a period of 6 months in 2001.

HASDM difficulties at high latitudes, and existence of density cells

Existing empirical density models do not adequately account for dynamic changes in neutral density, leading to errors in predicted satellite positions. The limitations in the empirical models include the inadequacy of the solar EUV/UV flux specification when using the 10.7 cm radio flux (F10.7 index) as input to the models in lieu of measured EUV irradiances. Another source of variability is the effect of diurnal and semidiurnal tides propagating up from the lower atmosphere. However, the major discrepancies between empirical models and data are at high latitudes, where extreme density variability is caused by the varying auroral inputs. There is still much to be learned about the behavior of the high latitude composition and density, and in this report we report a modeling study that explores and discusses some of their basic characteristics. Specifically, we report the results of numerical experiments to characterize, in terms of density "cells", the thermospheric density response to different levels of magnetic activity. We then explore, for the first time, the composition variations underlying the density cells. Finally, we predicted what are the likely UV signatures of these composition variations, including their IMF By dependence, and we showed how they might be observed with UV imagers that are being flown today.

The study used a 3-D fully coupled global model of the ionosphere-thermosphere system, called the Advanced SPace Environment (ASPEN) Thermosphere Ionosphere Mesosphere Electrodynamics General Circulation Model (TIMEGCM) with heritage in the long line of global models developed at the National Center for Atmospheric Research (NCAR).

4.1.1 Scientific Background

There have been numerous studies of the thermospheric compositional and density response to various stimuli. These were mostly a form of exploratory science, based on sparse satellite data. Even when measurements were available from the Atmosphere Explorer (AE) and Dynamics Explorer-1 (DE-1) satellites, the atmospheric drivers were not generally measured. Seasonal effects were studied by Mauersberger et al. (1976a,b) and by Mayr and Harris (1977). Recently, Fuller-Rowell et al (1998) suggested a mechanism to explain semi-annual variations in the thermospheric composition and density distribution. Their mechanism was called the "thermospheric spoon". They suggested that the global-scale interhemispheric transport at solstice acts like a giant spoon to mix the major species, although their CTIM model was unable to confirm this mechanism.

There have been many reports of storm effects on composition, including detailed modeling studies (e.g. Mayr et al., 1973; Burns et al., 1991, 1995a,b; Fuller-Rowell et al., 1994, 1996), and others based on the AE and DE satellites (e.g. Hedin et al., 1977; Miller et al., 1990). Much of this work was summarized by Buonsanto (1999). Magnetic storms and substorms cause major changes in the compositional distribution of the thermosphere. Crowley *et al.* [1989] showed how changes in thermospheric composition develop during storms and how Joule heating leads to upwelling of nitrogen-rich air which is transported to lower latitudes by equatorward winds on the nightside. Corotation then carries the oxygen-depleted air onto the dayside. Burns *et al.* [1991] described simulations that revealed upwelling and downwelling neutral winds as the primary mechanism causing the large enhancements of O relative to N_2 on the nightside in the winter hemisphere. Modeling by Fuller-Rowell *et al.* [1996] demonstrated the seasonal dependence of these processes and their effect on ionospheric electron densities.

The variations in thermospheric temperature, density, and composition have been captured in empirical models such as Jacchia (1970; 1974), in the Mass Spectrometer Incoherent Scatter Radar (MSIS) series of models of Hedin et al. (1977, 1991, 1996), and most recently in the NRLMSISE-00 model (Picone et al., 2002).

As mentioned above, the major discrepancies between empirical models and data are at high latitudes, where extreme density variability is caused by the varying auroral inputs. We have shown, in the past, that a first principles model driven by appropriate inputs can simulate the high latitude density features (Crowley et al., 1989a,b; 1995; 1996a,b) observed by satellites near 200 km altitudes. Cellular structures in the high latitude neutral density of the lower thermosphere were discovered by Crowley et al. (1989 a,b). The detailed morphology of the cells was described for solar minimum conditions by Crowley et al. (1996a). Crowley et al. (1996b) found conclusive evidence of the cellular structures in satellite density measurements from 200 km altitudes. Schoendorf and Crowley (1996) demonstrated how an 'anomalous' density decrease at high latitudes during a magnetic storm could be explained in terms of the formation of a low density cell in the dawn sector. The morphology of the cells for solar maximum was described by Schoendorf et al. (1996a). The mechanisms driving these cells have not been fully explained (e.g. Schoendorf et al., 1996b). The cell-like structures have also been simulated using the model of Fuller-Rowell et al. (1999). Caspers and Prolss (1999) used data to show evidence of the cells.

What we have learned from the previous studies is that the upper atmosphere is highly variable, being directly driven by three types of variable inputs: (a) the high latitude convection and auroral precipitation, (b) variability in the solar EUV, and (c) by tides and gravity waves propagating up from below. Modeling of this variability is extremely challenging because our knowledge of the inputs is incomplete, and their specification requires copious amounts of data. In spite of this previous work, there remain many important science questions to be addressed regarding the atmospheric response to geomagnetic activity. In this report, we begin to explore the variability of the high latitude inputs and the atmospheric response. Most models do not even try to accurately represent all the atmospheric drivers. However, in the current era of highly developed global 3-D fully coupled first principles models, several groups have attempted to specify all the inputs, using a variety of approaches (e.g. Fuller-Rowell et al., 1984; Roble et al., 1987; Crowley et al., 1989 a,b). In this study, we utilize a global 3-D first principles model known as ASPEN, which is based on the NCAR Thermosphere Ionosphere Mesosphere Electrodynamics General Circulation Model (TIMEGCM).

4.1.2 Thermosphere Ionosphere Mesosphere Electrodynamics General Circulation Model

Thermospheric General Circulation Models (TGCMs) were developed by the National Center for Atmospheric Research (NCAR) beginning in the early '80s to study the global temperature, circulation, and chemical structure of the thermosphere and its response to solar and auroral activity. A 3-D coupled thermosphere-ionosphere general circulation model (TI-GCM) was developed by Roble et al., (1988), and extended to include self-consistent electrodynamic interactions (TIE-GCM) between the ionosphere and thermosphere (Richmond et al. 1992). The model now extends down to 30 km, to include the mesosphere and upper stratosphere and is known as TIME-GCM (Roble and Ridley, 1994). It predicts winds, temperatures, major and minor composition, electron densities and electrodynamic quantities globally from 30 km to about 600 km altitude. The standard NCAR model uses a fixed geographic grid with a 5° x 5° horizontal resolution, and a vertical resolution of a half pressure scale height. (Recent versions of the TIMEGCM can also be run with a 2.5° horizontal resolution and a quarter scale height vertical resolution). The model time-step is typically 2-3 minutes, but rapid changes and storms usually require 1 minute time-steps, to maintain model stability.

The codes were initially developed at NCAR for a CRAY Supercomputer environment. Recently, the TIME-GCM code was ported to SwRI where it now runs in a distributed parallel computing environment, and is called the Advanced SPace ENvironment (ASPEN) TIMEGCM. The new code runs on the SwRI Distributed Computing Facility (DCF) which consists of 50+ high-end workstations connected by a dedicated high-speed ATM network (Freitas, 1995a,b,c), and on the SwRI Beowulf cluster, consisting of 32 high-end PCs. The ASPEN code has been thoroughly tested and validated to ensure it produces the same results as the NCAR codes, given the same inputs, to within numerical accuracy of the personal computers.

The TIME-GCM has played an important role in understanding the characteristics of the upper atmosphere. An important part of the NCAR TIMEGCM success has resulted from its detailed input specification. The inputs required by the TIME-GCM include the solar flux at 57 key wavelengths, parameterized by the $F_{10.7}$ flux. Typically the $F_{10.7}$ flux is available once per day, so short-term variability such as flare effects are not captured with any fidelity. However, day-to-day variability and longer-term effects like the 27 day solar rotation effect, and 11 year solar cycle are well reproduced. Until recently, these limitations have been adequate.

Other inputs required by the TIME-GCM include high latitude particle precipitation and electric fields. Roble and Ridley (1987) developed an analytical formulation of the auroral oval, and introduced the use of the Heelis convection model (Heelis et al, 1982). The Heelis model provided an analytical formulation for the shape of the potential pattern, including distortions from the effect of the IMF by component. The magnitude of the potential had to be specified, and was usually estimated from an empirical relationship with the Kp or Hemispheric Power (Hp) index. Other global models have used (and still use) Heppner-Maynard potential patterns (Heppner and Maynard, 1987).

The Roble and Ridley (1987) formulation of the auroral oval and associated particle precipitation has been used with great success. This formulation required some way of driving the auroral radius, particle flux, and energy as a function of magnetic local time and latitude. Usually the driver was the cross-cap potential, which was unknown, and had to be derived from an empirical relation with an index such as Kp or hemispheric power (Hp). Other global models have used measured particle climatologies driven by an index such as Hp (e.g. Fuller-Rowell et al, 1994). In general, the tides are specified from a tidal climatology at the lower boundary and

propagate up through the model domain, although they can be tuned for specific dates if sufficient tidal data are available.

The quality of the model inputs determines the quality of the outputs. And different classes of model studies have different requirements. The use of indices such as Kp and Hp limits the cadence and fidelity of the input drivers to the models, with a consequent loss of fidelity in the model predictions. To help overcome this limitation, Crowley et al. have used the Weimer (1996) model to derive values of cross-cap potential from 1-minute IMF data measured by the ACE satellite (e.g. Crowley et al., 2003; Lima et al., 2003). However, they still used the Heelis potential distribution, and the Roble et al (1987) auroral oval specification. For the study of global and low-latitude effects, this combination results in reasonably accurate simulations, but the approach results in limited improvement for detailed localized studies, especially at high latitudes.

Realizing these limitations, Crowley et al. (1989a, b) were the first to use assimilated electric fields and auroral precipitation specified by the Assimilative Mapping of Ionospheric Electrodynamics (AMIE) technique of Richmond and Kamide (1988) to drive a global thermosphere-ionosphere model. By using the AMIE fields, they were able to obtain much better agreement between the observed and modeled atmospheric responses. In fact, these new simulations were so accurate that they led to the discovery of an important structure in the high latitude neutral density and composition (Crowley et al., 1995, 1996a,b; Schoendorf and Crowley, 1995; Schoendorf et al., 1996a, 1996b). The use of AMIE as a driver for the TIMEGCM at NCAR has continued to the present day (e.g. Emery et al., 1996), and was recently implemented at SwRI.

4.2. RESULTS

In this report, we present the results of numerical experiments using the NCAR-TIMEGCM, to simulate quiet, moderate, active and severe storm conditions for solar maximum. Solar maximum conditions were selected because the DE mission took place at solar maximum, and the current era of ultraviolet imagers has begun at solar maximum. The quiet, moderate, active and severe storm conditions were simulated using cross-polar cap potentials of 30, 60, 90 and 120 kV, with appropriate hemispheric power inputs. Each simulation was run to a diurnally reproducible state with the cross-cap potential constant for five days. To investigate the effect of the IMF By component on the density and composition cells, the simulations were repeated with By values of +7, 0 and -7 nT. This selection of 12 runs reveals the development of compositional changes in response to different By conditions for different magnetic activity levels. In Crowley et al., (1996) we showed that the cell behaviour is quite different above a transition height of about 170 km, and that the cell structure decays above about 350 km. Therefore, in this report we examine results at 140 km, 200 km. We present the results of equinox simulations, and the corresponding results for solstice will be presented and compared in a future study. The results of these simulations will provide guidance for the interpretation of satellite data, including ultraviolet images of the column O/N2 ratio.

4.2.1 Variations in the high latitude convection pattern

Figure 1 summarizes the variations in the northern high latitude convection patterns obtained from the Heelis et al. (1982) model for three different IMF By conditions and four levels of magnetic activity. These patterns were used to drive the model to diurnally reproducible

conditions. The outer latitude of the figures is 42.5°N. The cross-cap potential increases (from left to right) from 30 to 120 kV, and the IMF increases up the page from -7 nT to +7 nT. The figure shows potential patterns for each condition at 23UT (contours) with ion-drift vectors at 200 km superposed. The patterns would rotate around the geographic pole as a function of UT (not shown).

The effect of increasing the cross-cap potential in the Heelis (1982) model, is to increase the radius of the convection reversal boundary, which effectively increases the size of the cells, so their effects spread to lower latitudes. In each case, the potential difference is split 55%:45% between the dusk and dawn cells. The effect of changing the IMF By component is to rotate the angle of flow across the polar region. So for the 30 kV case, and By = -7, the flow is in the noon-midnight meridian, but for By = 0 and +7, it is rotated clockwise by 15° and 30°, respectively. It also rotates the angle of entry on the dayside from about 11 SLT to 14 SLT.

4.2.2 Variations in the high latitude density cells.

Figure 2 summarizes the high latitude density structure at 140 km altitudes, obtained from the diurnally reproducible runs driven by the corresponding convection patterns in Figure 1. The cross-cap potential again increases (from left to right) from 30 to 120 kV, and the IMF increases up the page from -7 nT to +7 nT. Note we only show the cell structure at 23 UT. Also note that each panel has its own color scale. This convention is used throughout the report because we are more interested in the relative magnitude of features for a given case, than in comparing cases. For all values of the potential, there are only two density cells at this altitude, as reported by Crowley et al. (1996) for solar minimum conditions, and by Schoendorf et al (1996a) for solar maximum conditions. However, there is a hint of a third cell - a high density cell in the midnight sector. The superposed vectors represent neutral wind flows at 200 km.

Our earlier papers showed that the density cells are a dynamical feature driven by high latitude momentum forcing, and they are organized in magnetic coordinates (like the electric potential pattern) rather than geographic coordinates. Thus, like the potential pattern, the density cells precess around the geographic pole in 24 hours. Because the potential patterns in Figure 1 tended to rotate clockwise as The IMF By component changed from +7 nT to -7 nT, one might expect the density cells to rotate similarly. In fact they do, as confirmed by Figure 2. The rotation is especially evident in the dawn cells, but it also shows up in the evening cells and in the rotation of the neutral wind pattern.

Figure 3 shows the corresponding density cell structure for 200 km altitudes. For 30 kV, the density structure consists of two cells, with a high density in the evening sector and a low density in the morning sector. When the potential increased from 30 to 60 kV, the two-cell pattern changed to a 3-cell pattern, with an additional high-density cell in the midnight sector. For 90 kV, a new low-density cell formed in the evening sector, making four distinct cells. This structure was intensified at 120 kV. This development is similar to the results reported by Crowley et al (1996). What is new in Figure 3 is the intensification of the structure at 120 kV, and the rotation of the cell pattern as By is changed from +7 nT to -7 nT. The effect of the IMF By component is to rotate the cell structure in the clockwise direction for increasingly positive By. This mimics the rotation of the convection pattern described in Figure 1.

4.2.3 Composition variations

The high latitude composition structure corresponding to the densities in Figure 2 is summarized in Figures 4 and 5, for molecular nitrogen and in Figures 6 and 7 for atomic oxygen, respectively. Comparison of Figures 2 and 4 (or 3 and 5) reveals that the molecular nitrogen structure essentially mimics the density structure at altitudes from 140 to 200 km. This is because the nitrogen ranges from 75% of the atmosphere at 140 km, to 50% at 200 km. Thus, at 140 km, the N2 structure is virtually indistinguishable from the structures in the neutral density discussed above. There is also a significant similarity between the density and N2 structures at 200 km, shown in Figures 3 and 5. However, we note that the N2 compositional cells are clearer and more distinct in Figure 5 than the corresponding density cells in Figure 3. This is because the N2 cells do not blend into lower latitude enhancements present in the density distribution.

Figures 6 and 7 depict the corresponding atomic oxygen structure at 140 and 200 km. The atomic oxygen structure is very different from the N2 structure. In both figures, the O tends to have a simpler structure, consisting of a depletion in the polar region, with a minimum in the dawn sector. However, there is an O enhancement in the post-noon sector, especially for the 120 kV case, that appears to mimic the N2 enhancement. Unlike the N2, the overall O structure is substantially the same at 140 and 200 km.

4.2.4 Possible UV signatures of composition variations

The brightness of the FUV dayglow is directly related to the ratio of the column integrated concentrations of O and N_2 ([O]/[N_2]) in the thermosphere. Therefore the column integrated O/N_2ratio ($\Sigma O/N_2$)is the key parameter to determine whether the high latitude density cells and the corresponding composition variations will be detectable in the FUV. Figure 8 depicts the column integrated O/N_2ratio corresponding to the previous figures. The height integration was done from 135 km to about 600 km. The figure shows that the $\Sigma O/N_2$ is generally a circular depression in the polar region, reflecting the fact that O is generally depleted throughout the polar cap. There is a tendency for $\Sigma O/N_2$ to show a minimum on the dawnside of the polar cap, again reflecting the fact that O is lowest in that sector.

There is a distinct By effect in the $\Sigma O/N_2$, and the entire pattern appears to rotate anticlockwise as By changes from +7 to -7 nT. The rotation is closely related to the potential pattern rotation, as we shall see later. We also note that the depth and the horizontal extent of the depletion grow as the cross-cap potential increases.

4.2.5 Relationships Between Column Integrated O/N2 Ratio and Neutral Density

Having determined that neutral density cells and the associated composition changes produce effects that should be observable in FUV images, it is necessary to determine the inverse problem: if a dayglow depletion is observed in the polar cap, what can be deduced about the underlying neutral density structure? The most pressing questions are:

a) Does the location and horizontal extent of the modeled O/N2 depletion relate to the location and horizontal extent of the underlying density cells?

b) Does the magnitude of the O/N2 depletion relate to the magnitude of the density cell structure?

Both questions can be answered in a theoretical framework by using the model simulations alone. The first question can be answered by comparing the modeled column O/N2 ratio

distribution with the density distribution at different altitudes. In this study, our goal was to obtain a qualitative estimate of the relationships. A quantitative analysis will be provided in a future study using spatial correlation of the distributions.

We note that the density cell structure varies with altitude. Therefore, the $\Sigma O/N_2$ distribution is not obviously correlated with the density structure at all heights in the same way. The fact that the $\Sigma O/N_2$ is integrated in altitude, and the largest contributor is at altitudes near 140 km, means that the $\Sigma O/N_2$ is most likely to correlate with density and compositional changes at 140 km. In fact, the O/N_2 ratio for individual altitudes of 140km and 200 km in Figures 9 and 10, shows that the distributions at the two heights are very similar, and both show evidence of rotation with By.

In Figure 11, we show for the potential = 60 kV and By=+7 nT case the longitudinal relationship between the centers of the dawn low-density cell, the maximum potential (dawn), and the minimum in the $\Sigma O/N_2$ as a function of UT. We also show a dotted line representing the longitude of 6LT to guide the eye. It is readily apparent that the minimum in the potential pattern is generally rotated westward by about 5-90° of longitude from 6LT. The minimum in $\Sigma O/N_2$ is generally rotated eastward by 10-50° from the potential minimum. This graph provides the first quantitative relationship between the observable $\Sigma O/N_2$ and the potential pattern which drives the density cells. The figure also shows the locations of the dawn minimum in the density cells at 140 km, and the dawn minimum in N2 and O. The latter three are closely correlated, and each is rotated to the east of the minimum in the $\Sigma O/N_2$, by 5-40° of longitude. (The figure also shows the latitudes of the minima, which will not be discussed here). Similar results were obtained for all cases, and for both 140 and 200 km altitudes. There appears to be a predictable relationship between the dawn minimum of the potential, the density, the N2, the O and the $\Sigma O/N_2$ for each altitude.

The second question can be answered independently of the first by examining the magnitude of the O/N2 depletions and the density perturbations. In the past, Crowley et al. (1996a) showed that the density perturbations increased as a function of Kp and cross-cap potential used to drive the model. A similar analysis was performed in this study, and confirmed the earlier results. In a future study, the relationship will be obtained for the composition perturbations at different altitudes, and for the integrated O/N2 ratio.

4.2.6 Experimental Confirmation of Relationships Between Column Integrated O/N2 Ratio and Neutral Density

Having answered the questions based on the simulations, the results must be applied to the DE data, using realistic simulations as a guide. Images from the DE-1 satellite were selected having clear polar cap brightness depletions. Then the location, extent and magnitude of the brightness depletions observed by DE-1 were compared with the density perturbations measured *in-situ* by the DE-2 spacecraft. Figure 12 shows an example of the DE-2 O and N2 measurements as a function of UT for part of a single orbit during a magnetically active day in February 1983. We developed a simple correction for the DE-2 data to account for the altitude variation of the satellite during its elliptical orbit. This makes it easier to identify significant density perturbations, because the exponential changes introduced by the altitude variation have been removed. The corrected densities of O and N2 are represented by the dotted lines. The corresponding latitudes, altitudes, etc are shown in the other panels. Near the south polar region, the satellite encountered a strong latitudinal structure corresponding to density cells at altitudes of about 250 km.

We have examined DE-1 images corresponding to many such passes of DE-2. There is ample evidence of the density cells in the DE-2 data, but it is difficult to correlate them with specific depletions in the FUV brightness, such as that shown in Figure 13 (after Immel et al., 2001). More work is needed to quantify these relationships in the data, using model simulations as a framework for the comparisons. The column O/N2 ration from the corresponding TIMEGCM simulation will be generated for comparison with the DE-1 image. The DE-2 *in-situ* measurements of the temperature, O, and N2 will be used to validate the model simulations to determine whether the model accurately predicts the composition variations observed by DE-2. If the model accurately predicts the DE-2 composition, it must also accurately predict the neutral density, so the modeled $\Sigma O/N_2$ can be related to the modeled density cells, which can in turn be related to the observations. The best candidates are the December 1982 and Jan-Feb 1983 period, when DE-2 obtained good images of the southern high latitudes, and DE-1 was in a relatively low altitude (250-350 km) orbit that was beginning to circularize.

4.3 DISCUSSION

In recent years, models of the coupled thermosphere-ionosphere system have been developed that identify the major contributors to the aeronomy of the upper atmosphere. Relatively little work has been done to validate the global models with large ionosphere-thermosphere data sets, or to establish what are the shortcomings of the models and how they can be improved. Observations of the neutral composition and densities were unavailable for most of the space era, and even when they were available from the AE and DE satellites, the atmospheric drivers were not generally measured. In the present era, NASA has access to copious thermospheric density data from the GRACE and CHAMP accelerometers. In addition, ultraviolet imagers are currently in orbit on the NASA-TIMED and Air Force DMSP satellites. Finally, new tools like the Air Force Space Command's HASDM have emerged that use spacecraft orbits to correct density calculations, and yield density values with increased spatial and temporal resolution for drag computations (Storz et al., 2002; Casali and Barker, 2002; Wise et al., 2002). It is also possible to specify many of the thermospheric drivers with unprecedented accuracy. Solar and thermospheric observations from TIMED provide data with which to improve both the EUV specification and the neutral density (and temperature) responses to EUV variability. The present study will lead to improvements in the first-principles models, and make them suitable for eventual use in modeling the weather and climate of the ionosphere and thermosphere. More importantly, it has yielded results that could be incorporated into quasi-empirical models used routinely by Air Force personnel. It could also be incorporated into the HASDM analysis.

We have initiated discussions with HASDM personnel in Colorado Springs, and we are participating in the DMSP neutral density and dayside ionosphere Cal-Val efforts. We are also collaborating with the CHAMP and GRACE missions, which provide precise accelerometer and neutral density data. As a follow-on to the work reported here, we plan to compare CHAMP/GRACE density data with FUV images obtained from the GUVI instrument on NASA's TIMED mission and the DMSP SSUSI instrument.

5. PERSONNEL SUPPORTED

The PI, Dr. Geoff Crowley was the only SwRI staff member supported under this effort.

6. PUBLICATIONS

Crowley, G. and C. Hackert, **Quantification of High Latitude Electric Field Variability,** *Geophys Res. Lett.*, 28, 2783-2786, 2001.

Immel, T. J., G. Crowley, J. D. Craven, **Dayside enhancements of thermospheric O/N2 following a magnetic storm onset,** *J. Geophy. Res.,* 106, 15471-15488, 2001.

Paxton, L. J., D. Morrison, Douglas, J. Strickland, M. G. McHarg, H. Kil, G. Crowley, A. B. Christensen, and C. I. Meng, **The Use of Far Ultraviolet Remote Sensing to Monitor Space Weather**, Adv. Space Res., in press, 2001.

Immel, T., G. Crowley and J.D. Craven, The Importance of High Latitude Inputs in Correctly Modeling the Magnitude and Extent of Thermospheric Storms, Adv. Space Res., submitted, 2003.

Crowley, G., and C. Hackert, Thermospheric Density and Composition Response to the IMF By Component, to be submitted to J. Geophys. Res., 2004.

7. INTERACTIONS/TRANSITIONS

a) Participation/presentations at Meetings (most recent listed first)

L.J. Paxton, Y. Zhang, H. Kil, D. Morrison, B. Wolven, J. Baker, R. Greenwald, and G. Crowley, **Magnetosphere-Ionosphere-Thermosphere Coupling as Viewed by the NASA TIMED Mission**, submitted to Conference on Sun-Earth Connections: Multiscale Coupling in Sun-Earth Processes, Kona, Hawaii, February 9-13, 2004

Paxton, L. J., Y. Zhang, G. Crowley, R. DeMajistre, H. Kil, T. Kusterer, D. Morrison, B. Wolven, C. I. Meng, A. B. Christensen, M. Weiss, W. Wood,
Space Weather in the ITM: The May-June 2003 Storm and NASA TIMED/GUVI Observations and TIMEGCM Model Results,
submitted to Fall AGU Meeting, San Francisco, CA, Dec. 2003

Sharber, J., R. A. Frahm, M. Wüest, G. Crowley, K. Jennings,
Empirical Modeling of Global Energy Input During the April, 2002 Storms
submitted to Fall AGU Meeting, San Francisco, CA, Dec. 2003

J. H. Yee, E. R. Talaat, G. Crowley, R. Roble,
Atmospheric Effects of Solar/Geomagnetic Disturbances: the Role of Initial Atmospheric States,
submitted to Fall AGU Meeting, San Francisco, CA, Dec. 2003

Meier, R. R., D. J. Strickland, J. M Picone, A. B. Christensen, L. J. Paxton, D. Morrison, H. Kil, J. Bishop, D. Drob, J. D. Craven, G. Crowley, R. L. Walterscheid, S. Avery, C. I. Meng,
Retrieval of thermospheric temperature and N2, O and O2 concentrations from GUVI limb scans

submitted to Fall AGU Meeting, San Francisco, CA, Dec. 2003

Craven, J. D., D. J. Strickland, R. R. Meier, G. Crowley, A. B. Christensen, L. J. Paxton, D. Morrison, S. K. Avery, C. I. Meng, P. R. Straus, C. M. Swenson, R. L. Walterscheid,
Search for Thermospheric Composition Changes in the Morning Sector near Local Midnight in Association with Intense Substorm Activity,
submitted to Fall AGU Meeting, San Francisco, CA, Dec. 2003

Makela, J. J., G. Crowley, M. C. Kelley, M. N. Nicolls, J. Chau,
Study of the Pre-Reversal Enhancement at the Jicamarca Radio Observatory using the ASPEN-TIMEGCM
submitted to Fall AGU Meeting, San Francisco, CA, Dec. 2003

Crowley, G., S. Yee, E. Talaat, C. Hackert, R. Roble,
Modeling of the Energy Balance in the Mesosphere and Lower Thermosphere
submitted to Fall AGU Meeting, San Francisco, CA, Dec. 2003

Meier, R. R., D. J. Strickland, J. M. Picone, A. B. Christensen, L. J. Paxton, D. Morrison, K. Kil, J. Bishop, D. Drob, J. D. Craven, G. Crowley, R. L. Walterscheid, S. Avery, C.-I. Meng
Retrieval of thermospheric temperature and N2, O, and O2 concentrations from GUVI limb Scans
submitted to Fall AGU Meeting, San Francisco, CA, Dec. 2003

Salah, J. E., L. P. Goncharenko, M. Vigil, S. P. Zhang, G. Crowley,
Observations of the April 2002 Storm Event by the Global Incoherent Scatter Radar Network,
EISCAT Workshop at SRI, August 2003

Makela, J., G. Crowley, Kelley
Comparison of TIMEGCM Winds and Drifts with Jicamarca, Areicabo, Millstone Hill and Other Radar Data for the May-June 2002 Period,
DMSP-SSUSI Cal./Val. Team Meeting, Applied Physics Lab, Laurel, MD. May 2003

Makela, J., G. Crowley, Kelley
Comparison of TIMEGCM Winds and Drifts with Jicamarca, Areicabo, Millstone Hill and Other Radar Data for the April 2002 Storm,
DMSP-SSUSI Cal./Val. Team Meeting, Applied Physics Lab, Laurel, MD. May 2003

Zhang, T., L. Paxton and G. Crowley
Comparison of TIMEGCM and MSIS Simulation with GUVI Σ O/N2 for the May-June 2002 Period
DMSP-SSUSI Cal./Val. Team Meeting, Applied Physics Lab, Laurel, MD. May 2003

Zhang, T., L. Paxton and G. Crowley
Comparison of TIMEGCM and MSIS Simulation with GUVI Σ O/N2 for the April 2002 Storm.
DMSP-SSUSI Cal./Val. Team Meeting, Applied Physics Lab, Laurel, MD. May 2003

Straus, P., G. Crowley, Reinish
Comparison of TIMEGCM Simulations with Ionsonde Data for the May-June 2002 Period DMSP-SSUSI Cal./Val. Team Meeting, Applied Physics Lab, Laurel, MD. May 2003

Straus, P., G. Crowley, Reinish
Comparison of TIMEGCM Simulations with Ionsonde Data for the April 2002 Storm.
DMSP-SSUSI Cal./Val. Team Meeting, Applied Physics Lab, Laurel, MD. May 2003

Crowley, G., C. Hackert, L. Paxton, T. Zhang, P. Straus, J. Makela
Development of Accurate Space Weather Simulations for May-June 2002 Period
DMSP-SSUSI Cal./Val. Team Meeting, Applied Physics Lab, Laurel, MD. May 2003

G. Crowley

Advances in Modeling the Thermosphere for April 2002
TIMED-GUVI Team Meeting, Alexander, CA April 2002, April 2003

Crowley, G.
Recent Advances in Space Physics: Observation and Simulation
University of Texas at Dallas, April 15, 2003

Hackert, Chris, Geoff Crowley, Larry J. Paxton, Paul Straus, Andrew Christensen, Daniel Morrison, Brian Wolven, Hyosub Kil, Yongliang Zhang, L. Goncharenko, J. Makela, Y. Sahai, O. de la Beaujardiere, Ching Meng, John Craven, Doug Strickland, Charles Swenson, Richard Walterscheid, Robert Meier, Susan Avery.
Space Weather Effects of the April 15-23 2002 Geomagnetic Storm
Spring AGU Meeting
EGS - AGU - EUG Joint Assembly, Nice, France, April 2003

Goncharenko, L., J. Salah, G. Crowley, A. Namgaladze, C. Fesen, G. Lu, M. Hagan, M. Codresku
April 2002 events: models vs. data
TIMED Science Working Group Meeting, Feb. 11-13, 2003, Johns Hopkins University

Crowley, G. L. J. Paxton, P. Straus, A. B. Christensen, D. Morrison, B. Wolven, H. Kil, Y. Zhang, L. Honcharenko, J. Makela, Y. Sahai, O. de la Beaujardiere, C. Meng, J. Craven, D. Strickland, C. Swenson, R. Walterscheid, R. R. Meier, S. Avery
Space weather effect of the April 15-23 2002 geomagnetic storm
TIMED Science Working Group Meeting, Feb. 11-13, 2003, Johns Hopkins University

Talaat, E. R., R. DeMajistre, L. Paxton, J.-H. Yee, L. P. Goncharenko, G. Crowley, S. M. I. Azeem, H. Kil, B. Shpynev, Q. Zhou, D. Morrison, B. Wolven, Y. Zhang, and A. B. Christensen,
Comparison of TIMED/GUVI inferred nighttime electron density with ionospheric observations and models,
TIMED Science Working Group Meeting, Feb. 11-13, 2003, Johns Hopkins University

P. R. Straus, L. J. Paxton, G. Crowley, S. Henderson, H. Kil, D. Morrison, C. Swenson, A. B. Christensen,
GUVI nighttime observations of the equatorial and mid-latitude ionosphere.
TIMED Science Working Group Meeting, Feb. 11-13, 2003, Johns Hopkins University

Seasonal variation of thermospheric composition as measured by TIMED/GUVI
Crowley, G., L. J. Paxton, A. Christensen, D. Morrison, Y. Zhang, Y. Kil, B. Wolven, D. Strickland, J. Craven, R. Meier, P. Straus, R. Walterscheid, C.-I. Meng, C. Swenson, S. Avery,
Analysis of TIMED/GUVI daytime limb scans
TIMED Science Working Group Meeting, Feb. 11-13, 2003, Johns Hopkins University

Christensen, A. B., S. Avery, J. Craven, G. Crowley, R. Meier, C.-I. Meng, D. Morrison, L. Paxton, C. Swenson, R. Walterscheid
Scientific objectives and early results from the Global Ultraviolet Imager (GUVI) on the TIMED models,
TIMED Science Working Group Meeting, Feb. 11-13, 2003, Johns Hopkins University

Meier, R. R., D. J. Strickland, A. B. Christensen, L. Paxton, D. Morrison, J. Craven, G. Crowley, R. Walterscheid, S. Avery, C-I Meng, J. Bishop, J. M. Picone, D. Drob,
Analysis of TIMED/GUVI Daytime Limb Scans
TIMED SWG, Johns Hopkins University, SPL, February 2003

Kil, H., L. J. Paxton, S. Su, B. C. Wolven, Y. Zhang, D. Morrison, C. Meng, A. B. Christensen, C. M. Swenson, G. Crowley, R. R. Meier, P. R. Straus, D. J. Strickland, S. K. Avery, J. D. Craven, R. L. Walterscheid
The Morphology of Equatorial Plasma Density Depletions Observed by GUVI
Fall AGU Meeting
San Francisco, CA, Dec. 2002

D. J. Strickland, A. Christensen, R. Meier, L. Paxton, D. Morrison, J. Craven, G. Crowley, R. Walterscheid, S. Avery, C. Meng
Products Derived From GUVI Dayglow and Auroral Data
Fall AGU Meeting
San Francisco, CA, Dec. 2002

Weiss, M. B, L. J. Paxton, R. J. Barnes, J. J. Eichert, W. C. Wood, D. Morrison, A. B. Christensen, D. J. Strickland, J. D. Craven, R. R. Meier, G. Crowley, S. K. Avery, C. I. Meng, P. R. Straus, C. M. Swenson, R. L. Walterscheid, B. C. Woven
Exploiting Web-Based Systems to Provide Interactive Interpretation, Access and Display of Far Ultraviolet Data from the Global Ultraviolet Imager (GUVI) on TIMED
Fall AGU Meeting
San Francisco, CA, Dec. 2002

M. G. Mlynczak, L. Paxton, J. Kozyra, T. Woods, T. Zurbuchen, G. Lu, M. Lopez-Puertas, F. J. Martin-Torres, J. M. Russell, G. Crowley, R. Picard
Energy balance in the sun-earth system during the Solar Storm Events of April 2002
Fall AGU Meeting
San Francisco, CA, Dec. 2002

S. Henderson, P. R. Straus, C. M. Swenson, H. Kil, A. Christensen, L. J. Paxton, G. Crowley, R. R. Meier, D. Morrison, J. D. Craven, D. Strickland, C. Meng, R. L. Walterscheid, S. Avery
A Quantitative Image Processing Approach To GUVI Observations Of The Equatorial Arcs.
Fall AGU Meeting
San Francisco, CA, Dec. 2002

B. Wolven, L. Paxton, D. Morrison, Y. Zhang, H. Kil, C. Meng, A. Christensen, P. R. Straus, R. Walterscheid, J. D. Craven, D. J. Strickland, R. R. Meier, G. Crowley, S. K. Avery, C. M. Swenson,
Thermospheric And Ionospheric Response To The Solar Flares Of April 2002 As Observed By The TIMED Global Ultraviolet Imager (GUVI)
Fall AGU Meeting
San Francisco, CA, Dec. 2002

O. de La Beaujardiere, G. Crowley, J. Makela, F. Rich, J. Retterer, D. Decker, W. Burke, B. Basu, T. Bullett, M. Kelley, L. McNamara, C. Huang, C. Valladares, P. Doherty,
The Global Ionosphere During The April 17 To 20, 2002 Magnetic Storm,
Fall AGU Meeting
San Francisco, CA, Dec. 2002

A. B. Christensen, D. J. Strickland, L. J. Paxton, D. Morrison, G. Crowley, R. R. Meier, J. D. Craven, C. I. Meng, C. M. Swenson, R. L. Walterscheid, S. K. Avery
Thermospheric Composition: GUVI Observations of O/N2
Fall AGU Meeting
San Francisco, CA, Dec. 2002

G. Crowley, L. J. Paxton, A. B. Christensen, D. Morrison, D. J. Strickland, J. D. Craven, R. Meier, P. Straus, R. Walterscheid, C. Meng, C. Swenson, S. Avery, C. Hackert
Seasonal Variation of Thermospheric Composition as Measured by TIMED/GUVI
Fall AGU Meeting
San Francisco, CA, Dec. 2002

J. Yee, G. Crowley
Scientific Results from the TIMED Mission I
Fall AGU Meeting
San Francisco, CA, Dec. 2002

A. B. Christensen, D. Strickland, L. Paxton, D. Morrison, G. Crowley, R. Meier, J. Craven, C. Meng, C. Swenson, R. Walterscheid, S. Avery, P. Straus
Global Ultraviolet Imager (GUVI): on –Orbit Performance and Initial Results
Fall AGU Meeting
San Francisco, CA, Dec. 2002

J. U. Kozyra, D. N. Baker, G. Crowley, D. S. Evans, X. Fang, R. A. Frahm, S. G. Kanekal, M. W. Liemohn, G. Lu, G. M. Mason, R. A. Mewaldt, L. J. Paxton, E. C. Roelof, J. D. Winningham
The Relative Atmospheric Impacts And Energy Inputs Of Precipitation Solar And Magnetospheric Ion And Electron Populations During The 17-24 April 2002 Events
Fall AGU Meeting
San Francisco, CA, Dec. 2002

L. J. Paxton, G. Crowley, Y. Zhang, B. Wolven, D. Morrison, H. Kil, R. DeMajistre, R. Barnes, M. Weiss, W. Wood, J. Echert, J. Kozyra, A. B. Christensen, S. Avery, J. Craven, R. Meier, C. Meng, P. Straus, D. Strickland, R. Walterscheid
GUVI/TIMED Observations During the April 14-24, 2002 Storm
Fall AGU Meeting
San Francisco, CA, Dec. 2002

J. D. Craven, D. J. Strickland, R. R. Meier, G. Crowley, A. B. Christensen, L. J. Paxton, D. Morrison, S. K. Avery, C. Meng, P. R. Straus, C. M. Swenson, R. L. Walterscheid
Search for thermospheric composition changes in the morning sector near local midnight in association with substorm activity
Fall AGU Meeting
San Francisco, CA, Dec. 2002

Y. Zhang, L. Paxton, D. Morrison, B. Wolven, H. Kil, C. Meng, A. Christensen, P. Straus, R. Walterscheid, G. Crowley, R. Meier, D. Strickland, J. Craven, S. Avery, C. Swenson,
Dayside auroras during storms of April 2002: TIMED/GUVI observations
Fall AGU Meeting
San Francisco, CA, Dec. 2002

R. Barnes, L. Paxton, M. Weiss, B. Wolven, A. Christensen, J. Craven, G. Crowley, S. Avery, R. Meier, C. Meng, P. Strauss, D. Strickland, C. Swenson, R. Walterscheid
Data visualization tools and techniques developed for the TIMED/GUVI instrument
Fall AGU Meeting
San Francisco, CA, Dec. 2002

E. R. Talaat, R. DeMajistre, L. Paxton, J. Yee, L. P. Goncharenko, G. Crowley, S. Azeem, B. Shypnev, Q. Zhou, H. Kil, D. Morrison, B. C. Wolven, Y. Zhang, A. Christensen,
Comparison of TIMED/GUVI inferred nighttime electron density with ionospheric observations and models
Fall AGU Meeting
San Francisco, CA, Dec. 2002

R. R. Meier, D. J. Strickland, A. B. Christensen, L. J Paxton, M. D. Morrison, J. D. Craven, G. Crowley, R. L. Walterscheid, S. K. Avery, C. I. Meng
Thermospheric composition derived from TIMED/GUVI limb scans
Fall AGU Meeting
San Francisco, CA, Dec. 2002

S. M. Baliey, G. Crowley, S. C. Solomon, D. N. Baker
The response to thermospheric nitric oxide to the geomagnetic storm April 2002
Fall AGU Meeting
San Francisco, CA, Dec. 2002

J. J. Makela, M. C. Kelley, G. Crowley, M. J. Nicolls, J. L. Chau, S. Gonzalez, Chris Hackert
Comparison of the TIMEGCM model to Jicamarca and Arecibo measurements during the April 2002 World Day observations
Fall AGU Meeting
San Francisco, CA, Dec. 2002

R. Frahm, G. Crowley, L. J. Paxton, C. Jackman, A. Christensen, D. Strickland, J. D. Winningham, J. Sharber, S. Avery, J. Craven, R. Meier, C. Meng, P. Straus, C. Swenson, R. Walterscheid,
Validation of the GUVI Auroral Radiance Measurements Using the UARS/PEM Instrument,
Fall AGU Meeting
San Francisco, CA, Dec. 2002

J. Kozyra and G. Crowley
Urgent Modeling Needs for the Living With A Star Programs
NASA Living With A Star Workshop
APL, Laurel, MD, Nov. 2002

G. Crowley,
Thermosphere Ionosphere Modeling and UV Imagers
NASA Living With A Star Workshop
APL, Laurel, MD, Nov. 2002

R. A. Frahm, G. Crowley, J. D. Winningham, J. R. Sharber and L. J. Paxton
April 18-24, 2002: PEM Observations of Atmospheric Energy Input and Ionization Rates Determined From Precipitation Charged Particles
AMS Meeting
San Antonio, TX Nov. 2002

G. Crowley, J. Olivero, C. Hackert, G. Thomas, J. Russell III, L. Gordley
H_20 Ice at the Mesopause HALOE Ice Saturation Regions and PMCs
AMS Meeting
San Antonio, TX Nov. 2002

G. Crowley, R. Frahm, J. D. Winningham
UARS PEM Observations for April 2002
TIMED-CEDAR Storms Workshop,
Haystack Observatory,
Westford, MA Oct 2002

G. Crowley, L. J. Paxton, P. Straus, A. Christensen, D. Morrison, L. Goncharenko, J. Makela, Y. Sahai, L. C. Lima, C. Meng, B. Wolven, H. Kil, Y. Zhang, J. Craven, D. Strickland, C. Swenson, R. Walterscheid, R. Meier, S. Avery
Space Weather Effects of the October 2002
TIMED-CEDAR Storms Workshop,
Haystack Observatory,
Westford, MA Oct 2002

G. Crowley, C. Freitas, M. Bullock, D. Boice, L. Young, R. Gladstone, R. Link, W. Huebner,
Development of a new Mars atmosphere model
Division of Planetary Sciences (DPS) of the American Astron. Society
Birmingham AL, Oct. 2002

G. Crowley, L. J. Paxton, P. Straus, A. Christensen, D. Morrison, L. Goncharenko, J. Makela, Y. Sahai, L. C. Lima, C. Meng, B. Wolven, H. Kil, Y. Zhang, J. Craven, D. Strickland, C. Swenson, R. Walterscheid, R. Meier, S. Avery
Space Weather Effects Of The April 16-23 2002 Geomagnetic Storm
COSPAR, Houston, TX Oct. 2002

P. R. Straus, G. Crowley, L. J. Paxton, A. B. Christensen, D. Morrison, H. Kil
TIMED/GUVI Observations of the Equatorial Anomaly: First-Principles Model Comparisons
COSPAR, Houston, TX Oct. 2002

T. J. Immel, G. Crowley, J. D. Craven,
The Importance of High Latitude Inputs in Correctly Modeling the Magnitude and Extent of Thermospheric Storms
COSPAR, Houston, TX Oct. 2002

G. Crowley
Living With A Star Targeted Research And Technology Definition Team
Ionosphere Thermosphere Coupling: Review of Modeling Status
College Park, MD Sept. 2002

G. Crowley
Dayside Ionospheric Effects of April 2002 Storm
SSUSI Cal/Val Team Meeting
Applied Physics Lab., Columbia, MD, Aug. 2002

G. Crowley
Atmospheric effects of the April 2002 Storm Simulated by the TIMEGCM
TIMED Storm Workshop, APL, Maryland, August 2002

G. Crowley, R. Frahm, J. Winningham,
UARS-PEM Observations for April 2002 Storm
TIMED Storm Workshop, APL, Maryland, August 2002.

G. Crowley
Dayside Ionospheric Effects of April 2002 Storm
SSUSI Cal/Val Team Meeting
Boulder, CO June 2002

G. Crowley, L. J. Paxton, P. Straus, A. Christensen, D. Morrison, C. Meng, B. Reinisch, R. Heelis, B. Wolven, J. Kil, Y. Zhang, J. Craven, D. Strickland, C. Swenson, R. Walterscheid, R. Meier, S. Avery,
Space Weather Effects of the April 16-23 2002 Geomagnetic Storm
CEDAR Meeting, Boulder, CO, June 2002.

G. Crowley, C. Hackert, M. Ruohoniemi,
Temporal and Spatial Variability of The High Latitude Electric Field
CEDAR Meeting, Boulder, CO, June 2002.

J. Bronn, G. Crowley, B. Fessler, E. Weigle, A. Eckhardt, C. Zeigler, K. Jennings, and G. Wene
TIDs Observed over Texas Using the TIDDBIT HF Doppler radar,
CEDAR Meeting, Boulder, CO, June 18, 2002.

Frahm, R., J. D. Winningham, J. R. Sharber, G. Crowley, R. Link, M. Wüest, J. Mukherjee, J. K. Jennings, A. Hudson, P. F. Gutierrez, and J.-P. Utter Löfgren,
Modeling of the Solar Wind Originated Energy Relevant to the Thermosphere/Ionosphere, Submitted to the 4th (Virtual) TIGER Meeting, May 2002.

Frahm, R., J. D. Winningham, R. Link, J. R. Sharber, G. Crowley,
UARS Climatology: Modeling of the Solar Wind Originated Energy Relevant to the Thermosphere/Ionosphere,
Submitted to the 4th (Virtual) TIGER Meeting, May 2002.

Christensen, A. B., L. J. Paxton, D. J. Strickland, R. R Meier, C. I. Meng, J. D. Craven, G. Crowley, S. K. Avery, R. L. Walterscheid, C. Swenson,
Scientific Objectives and Early Results from the Global Ultraviolet Imager (GUVI) on the TIMED Spacecraft,
Presented at Spring AGU, Washington, DC May 2002.

G. Crowley and B. Fessler,
TIDs Observed over Texas using the TIDDBIT HF Doppler Radar,
SwRI Division 16 Lunchtime seminar, May 23, 2002.

J. Olivero, G. Crowley, C. Hackert, G. Thomas, J. Russell, L. Gordley
Ice at the Mesopause: What Do HALOE Measurements Predict?
Fall Meeting of AGU
San Francisco, CA, December 2001.

G. Crowley, and C. Hackert
Quantification of High Latitude Electric Field Variability
Fall Meeting of AGU
San Francisco, CA, December 2001.

R. A. Frahm, J. D. Winningham,, J. R. Sharber, G. Crowley, and R. Link
The PEM Climatology: Version 3 Formulation
UARS Science Team Meeting
Washington, DC, Sept. 11-13, 2001

R. A. Frahm, J. D. Winningham, J. R. Sharber, G. Crowley, R. Link, M. Wuest, J. Mukherjee, J. K. Jennings, A. Hudson, P. F. Gutierrez, and J.-P. Utter Lofgren
Modeling of the Solar Wind Originated Energy Relevant to the Thermosphere/Ionopshere
3rd Thermospheric/Ionospheric Geospheric Research (TIGER) Symposium
Denver, CO June 2001

G. Crowley and C. Hackert
Temporal Variability in E-field, Conductance and Joule Heating
TIMED/GUVI Team Meeting
Boulder, CO April 22, 2001

b) Consultative/Advisory Functions

i) Served on DMSP-SSUSI Calibration and Validation Team. Dr. Paul Straus (Aerospace) leads this effort on behalf of the DMSP SPO. (Dr. Crowley was responsible for managing the SSUSI Ground Data Analysis System during his employment at JHU-APL). On the Cal-Val team he will perform TIMEGCM simulations to support the SSUSI Dayside algorithm.
ii) Invited to serve at CCMC advisory meeting in Hawaii (November 2001).
iii) Served on NASA GEC Science and Mission Definition Team (Meetings, Final Report).
iv) NSF CEDAR Proposal Review Panel (Aug/Sept 01)
v) Served on NASA Targeted Research and Technology (Theory and Modeling) Mission Definition Team (2002-2003)
vi) Served on NASA Living With A Star Management operations Working Group (2003-2005).
vii) NSF GEM-CEDAR Magnetosphere-Ionosphere Coupling Proposal Review Panel (September 2003)
viii) Invited to serve on DMSP SSUSI Neutral Density Cal-Val team (October 2003)

ix) Invited to be an associate of the NSF Center For Space Weather Modeling (CISM) led by Boston University (Fall 2003).
x) Reviewed proposals for NASA and NSF.
xi) Reviewed manuscripts for JGR, GRL, Ann. Geophys., Adv. Space Res., Radio Science

c) Transitions
Dr. Crowley was responsible for the development of a real-time version of the Assimilative Mapping of Ionospheric Electrodynamics at SwRI, through the help of Dr. Aaron Ridley. (Refer to Ridley, A.J., G. Crowley, and C. Freitas, **A statistical model of the ionospheric electric potential**, *Geophys. Res. Letters*, Vol. 27, No. 22, 3675-3678, 2000). This was transitioned in 2001 to NGDC in Boulder, under a separate contract to Dr. Ridley from Dr. Herb Kroehl.

8. NEW DISCOVERIES:

Listed above in Summary of Accomplishments by Task.

9. HONORS/AWARDS

- Promoted from "Principal Research Scientist" to "Staff Scientist" within SwRI.
- Invited to run for position of Secretary for the SPA section of the American Geophysical Union

10. BIBLIOGRAPHY

Buonsanto, M. J., Ionospheric Storms – A Review, *Space Sci. Reviews*, 88, 563-601, 1999.

Burns, A. G., T. L. Killeen, G. R. Cargnan, R. G. Roble, Large Enhancements In The O/N2 Ratio In The Evening Sector Of The Winter Hemisphere During Geomagnetic Storms, *J. Geophys. Res.*, 100, 14661-14671, 1995a.

Burns, A. G., T. L. Killeen, W. Deng, G. R. Cargnan, R. G. Roble, Geomagnetic Storm Effects In The Low-To-Middle-Latitude Upper Thermosphere, *J. Geophys. Res.*, 100, 14673-14691, 1995b.

Burns, A. G., T. L. Killeen, R. G. Roble, A Theoretical Study of Thermospheric Composition Perturbations During An Impulsive Geomagnetic Storm, *J. Geophys. Res.*, 96, 14153-14167, 1991.

Casali, S.J., and W.N. Barker, Dynamic calibration atmosphere (DCA) for the high accuracy satellite drag model (HASDM), Proceedings of the AIAA/AAS Astrodynamics Specialist Conference, Monterey, CA., August 2002, AIAA 2002-4888, 2002.

Caspers T., and G.W. Prolss, Thermospheric Density Cells at High Latitudes, Adv. Space Res., 21, 1999.

Crowley, G., L. J. Paxton, D. Morrison, A. Christensen, C. Hackert, Y. Zhang, H. Kil, Y. Sahai, L.C. Lima, P. Straus, B. Reinisch, C. Meng, B. Wolven, J. Craven, D. Strickland, C. Swenson, R. Walterscheid, R. Meier, S. Avery, J. Bronn, K. Jennings, L. Goncharenko, J. Makela, Space Weather Effects of the April 16-23 2002 Magnetic Storm, Submitted to Adv. Space Res., Feb 2003.

Crowley, G., J. Schoendorf, R.G. Roble, and F.A. Marcos, Cellular Structures in the High-Latitude Thermosphere, J. Geophys. Res., Vol. 101, 211-223, 1996a.

Crowley, G., J. Schoendorf, R.G. Roble, and F.A. Marcos, Neutral Density Cells in the Lower Thermosphere at High Latitudes, Adv. Space Res., Vol. 18, (3), 69-74, 1996b.

Crowley, G., J. Schoendorf, and F.A. Marcos, Satellite Observations of Neutral Density Cells in the Lower Thermosphere at High Latitudes, AGU Geophysical Monograph on the Upper Mesosphere and Lower Thermosphere, Vol. 87, 339-347, 1995.

Crowley, G., Emery B.A., Roble R.G., Carlson H.C. and Knipp D.J., Thermospheric Dynamics During The Equinox Transition Study I. Model Simulations for Sept 18 and 19, 1984, J. Geophys. Res., Vol. 94, 16925-16944, 1989a.

Crowley, G., Emery B.A., Roble R.G., Carlson H.C., Salah J.E., Wickwar V.B., Miller K.L., Oliver W.L., Burnside R.G. and Marcos F.A., Thermospheric Dynamics During The Equinox

Transition Study Of September 1984 II. Validation of the NCAR-TGCM, J. Geophys. Res., Vol. 94, 16945-16960, 1989b.

Emery, et al., The May 1996 substorm using POLAR images: Comparison of different data sets and empirical models, *EOS*, **77**, F613, 1996.

Fuller Rowell, T.J., T. Matsuo, M.V. Codrescu and F.A. Marcos, Modeling Thermospheric Neutral density Waves and Holes in response to High Latitude Forcing, Adv. Space Res., 24(11), 14447-1458, 1999.

Fuller-Rowell, T. J., M. V. Codrescu, R. G. Roble, and A. D. Richmond, How Does the Thermosphere and Ionosphere React to a Geomagnetic Storm?, Magnetic Storms, Geophysical Monograph 1998.

Fuller-Rowell, T. J., M. V. Codrescu, H. Rishbeth, R. J. Moffett and S. Quegan, On the Seasonal Response of the Thermosphere and Ionosphere to Geomagnetic Storms, *J. Geophys. Res.*, 101, 2343-2353, 1996.

Fuller-Rowell, T. J., M. V. Codrescu, R. J. Moffett and S. Quegan, Response of the Thermosphere and Ionosphere to Geomagnetic Storms, *J. Geophys. Res.*, 99, 3893-3914, 1994.

Fuller-Rowell, T. J., A two-dimensional, high-resolution, nested-grid model of the thermosphere, 1, neutral response to an electric field "spike", *J. Geophys. Res.*, 89, 2971, 1984.

Freitas, C.J., Perspective: Selected Benchmarks from Commercial CFD Codes, *Journal of Fluids Engineering,* Vol. 117, p. 7, 1995a.

Freitas, C.J., The End of Justification, The Beginning of Implementation, *Journal of Fluids Engineering,* Vol. 117, p. 7, 1995b.

Hedin, A. E., et al., Empirical wind model for the upper, middle, and lower atmosphere, J. Atmos. Terr. Phys., 58, 1421-1447, 1996.

Hedin, A. E., Extension of the MSIS Thermosphere Model Into the Middle and Lower Atmosphere, *J. Geophys. Res.*, 96, 1159-1172, 1991.

Hedin, A. E., P. Bauer, H. G. Mayr, G. R. Carignan, L. H. Brace, H. C. Brinton, A. D. Parks, and D. T. Pelz, Observations of Neutral Composition and Related Ionospheric Variations During a Magnetic Storm in February 1974, *J. Geophys. Res.*, 82, p3183, 1977.

Heelis, R. A., J. K. Lowell, and R. W. Spiro, A model of the high-latitude ionospheric convection patterns, *J. Geophys. Res.,* 87, 6339-6345, 1982.

Heppner, J.P., and N.C. Maynard, Empirical high-latitude electric field models, *J. Geophys. Res., 92*, 4467, 1987.

Jacchia, L. G., Variations in Thermospheric Composition: A Model Based on Mass Spectrometer and Satellite Drag Data, *J. Geophys. Res.*, 79, p1923, 1974.

Jacchia, L.G., "New Static Models of the Thermosphere and Exosphere with Empirical Temperature Profiles", SAO Report 313, May, 1970.

Lima, W., F. Becker-Guedes, Y. Sahai, P. R. Fagundes, J. R. Abalde, G. Crowley, and J. A. Bittencourt, Response of the Equatorial and Low-Latitude Ionosphere during the Space Weather Events of April 2002, 2003

Liu, J.F., R.G. France, and H.B. Wackernagel, An Analysis Of The Use Of Empirical Atmospheric Density Models In Orbital Mechanics, AAS/AIAA Astrodynamics Specialist Conference (Lake Placid, NY), August 1983.

Marcos, F.A., Accuracy of Atmosphere Drag Models at Low Satellite Altitudes, Adv. Space Res., 10(3), 417-422, 1990.

Mauersberger, K., D. C. Kayser, W. E. Potter, and A. O. Nier, Seasonal Variation of Neutral Thermospheric Constituents in the Northern Hemisphere, *J. Geophys. Res.*, 81, p7, 1976a.

Mauersberger, K., W. E. Potter, and D. C. Kayser, A Direct Measurement of the Winter Helium Bulge, *Geophys. Res. Lett.*, 3, 269-272, 1976b.

Mayr, H. G. and H. Volland, Magnetic Storm Characteristics of the Thermosphere, *J. Geophys. Res.*, 78, p2251, 1973.

Miller, N. J., L. H. Brace, N. W. Spencer, and G. R. Carignan, DE 2 Observations of Disturbances in the Upper Atmosphere During a Geomagnetic Storm, *J. Geophys. Res.*, 95, 21017-21031, 1990.

Picone, J. M., A. E. Hedin, D. P. Drob, and A. C. Aikin, NRLMSISE-00 Empirical Model of the Atmosphere: Statistical Comparisons and Scientific Issues, J. Geophys. Res., Paper No. 2002JA009430, In press, 2002.

Richmond, A. D., Ridley, E. C., Roble, R. G., A thermosphere/ionosphere general circulation model with coupled electrodynamics, *Geophys. Res. Lett.*, 19, 601-604, 1992.

Richmond, A. D., and Y. Kamide, Mapping electrodynamic features of the high latitude ionosphere from localized observations: Technique, J. Geophys. Res., 93, 5741-5759, 1988.

Roble, R. G., and E. C. Ridley, A thermosphere-ionosphere-mesosphere-electrodynamics general circulation model (time-GCM): Equinox solar minimum simulations (30-500 km), Geophys. Res. Lett., 21, 417-420, 1994.

Roble, R. G., T. L. Killeen, N. W. Spencer, R. A. Heelis, P. H. Reiff, and J. D. Winningham, Thermospheric dynamics during November 21-22, 1981: Dynamics Explorer measurements and thermospheric general circulation model predictions, J. Geophys. Res. 93, 209-225, 1988.

Roble, R. G., and E. C. Ridley, An auroral model for the NCAR thermospheric general circulation model (TGCM), *Ann. Geophys. Ser. A,* 5, 369-382, 1987.

Schoendorf, J., G. Crowley, R.G. Roble, and F.A. Marcos, Neutral Density Cells in the High Latitude Thermosphere -1. Solar Maximum Cell Morphology and Data Analysis, J. Atmos. Terr. Phys., Vol. 58, 1751-1768, 1996a.

Schoendorf, J., G. Crowley, and R.G. Roble, Neutral Density Cells in the High Latitude Thermosphere -2. Mechanisms, J. Atmos. Terr. Phys., Vol. 58, 1769-1781, 1996b.

Storz, M.F., B.R. Bowman and J.I. Branson, High Accuracy Satellite Drag Model (HASDM), AIAA/AAS Astrodynamics Specialist Conference (Monterey, CA), August 2002.

Weimer, D. R., A flexible, IMF dependent model of high-latitude electric potentials having "space weather" applications, Geophys. Res. Lett., 23, 2549-2552, 1996.

Wise, J.O., F.A. Marcos, B. Bowman, M.J. Kendra, and J.N. Bass, AFRL Neutral Density Support to HASDM, AIAA/AAS Astrodynamics Specialist Conference (Monterey, CA), August 2002.

Potential 200km 23UT

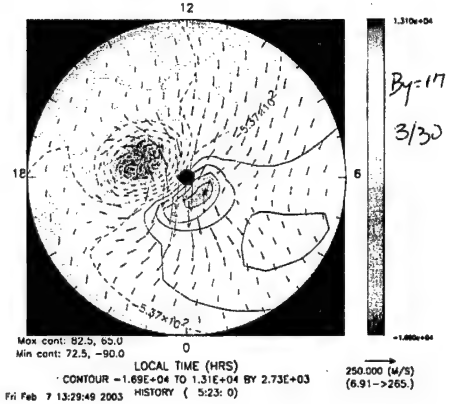

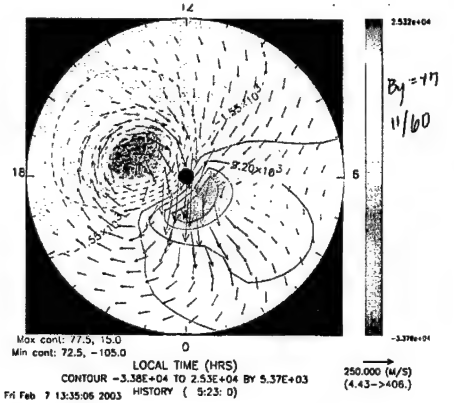

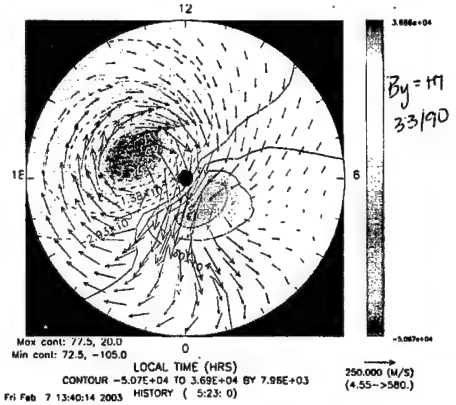

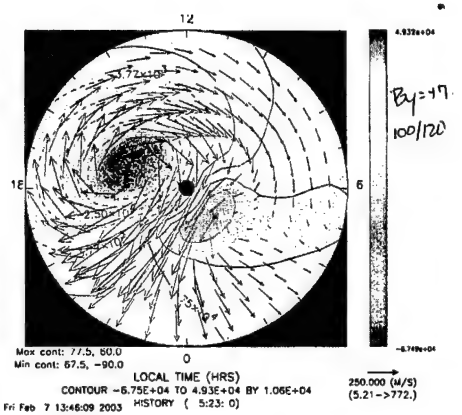

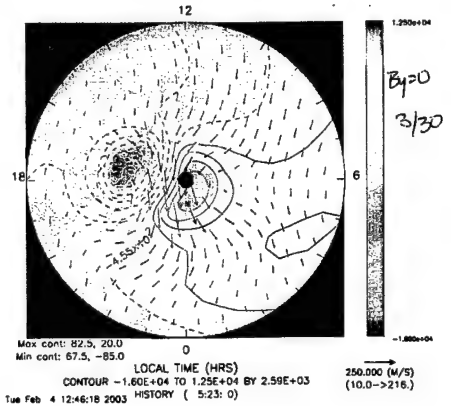

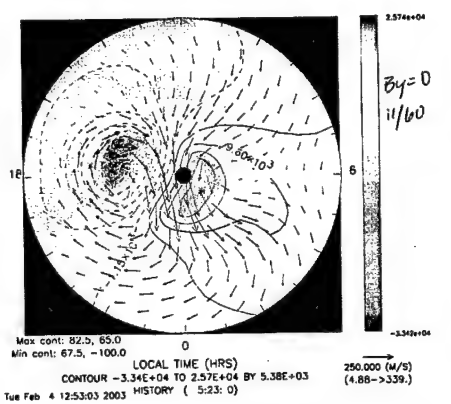

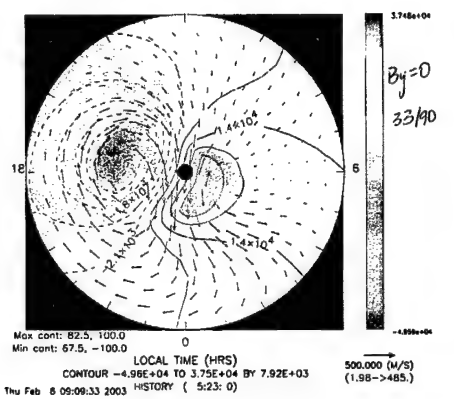

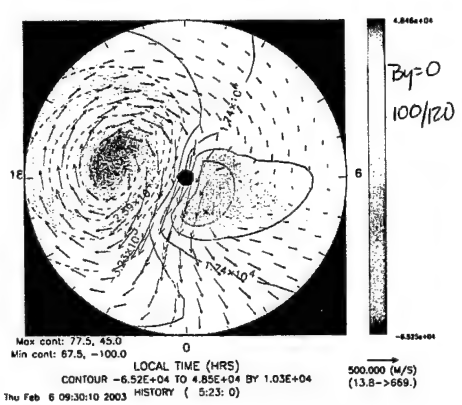

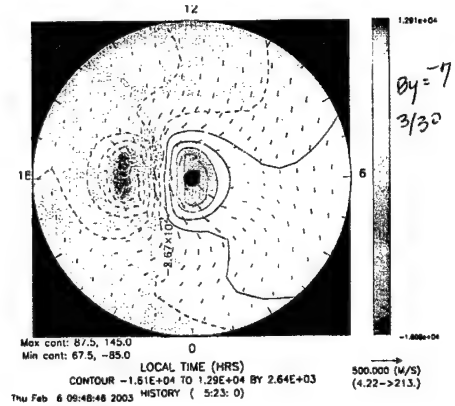

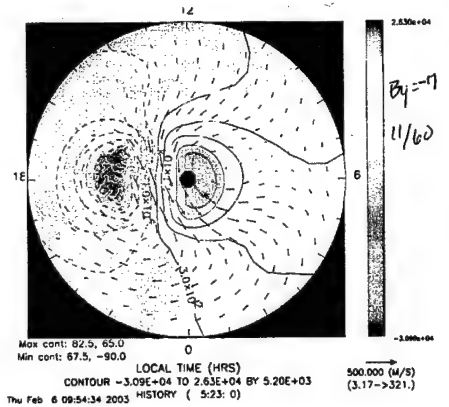

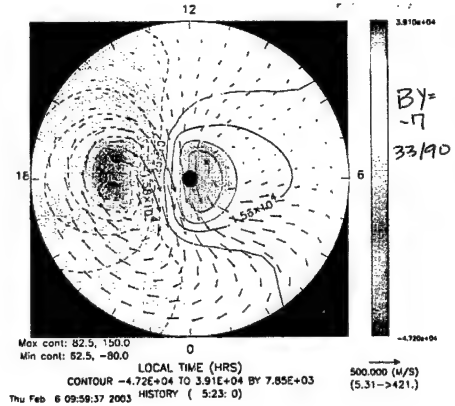

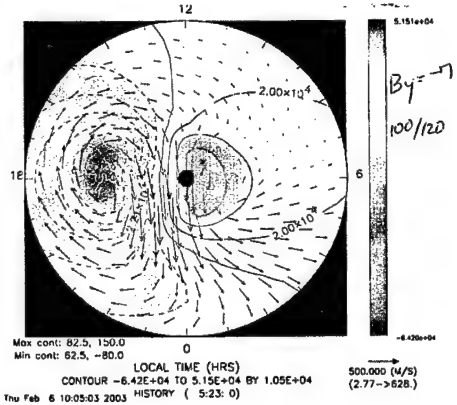

FIGURE 1

RHO 140km 23UT

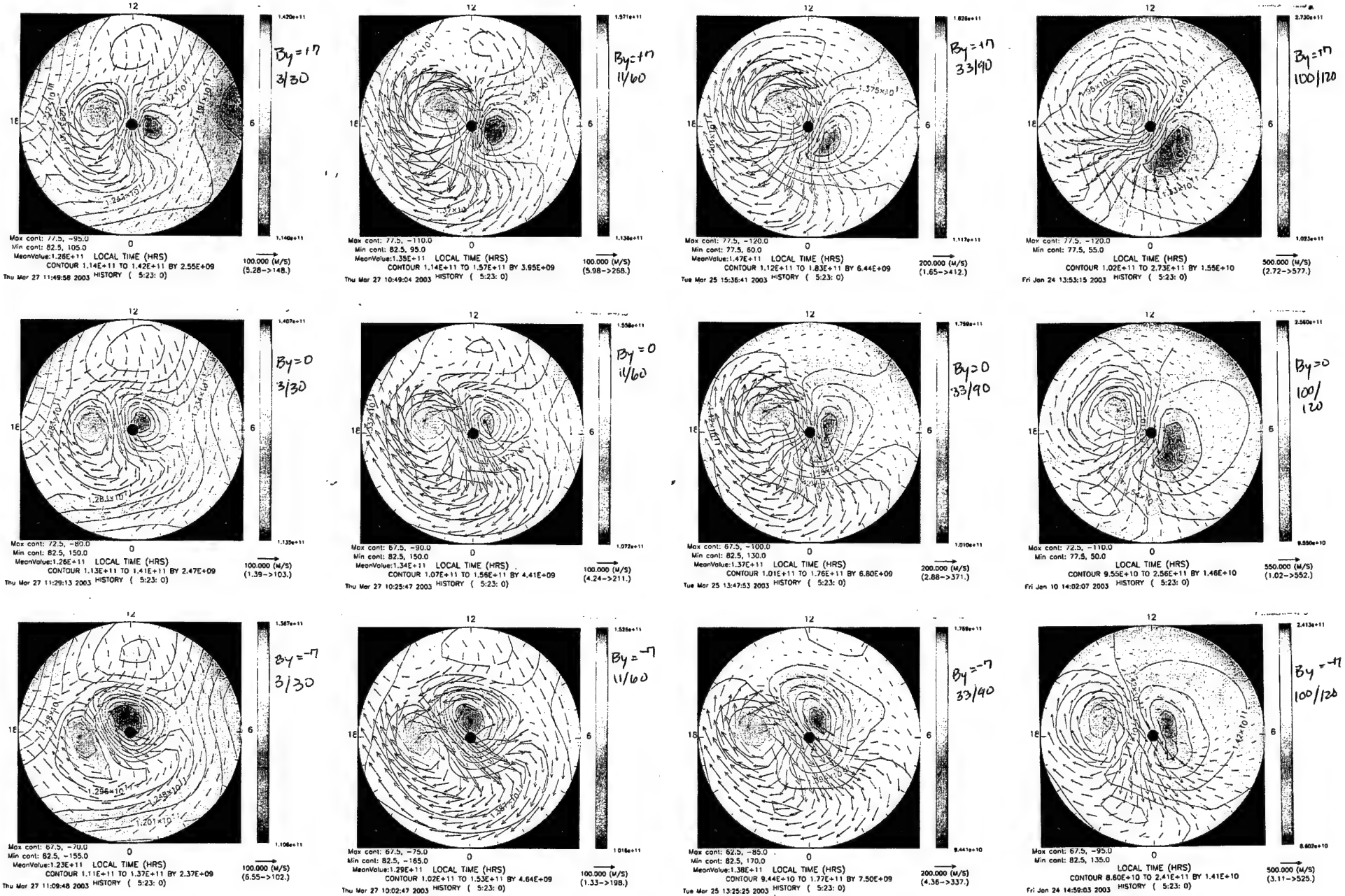

FIGURE 2

RHO 200km 23uT

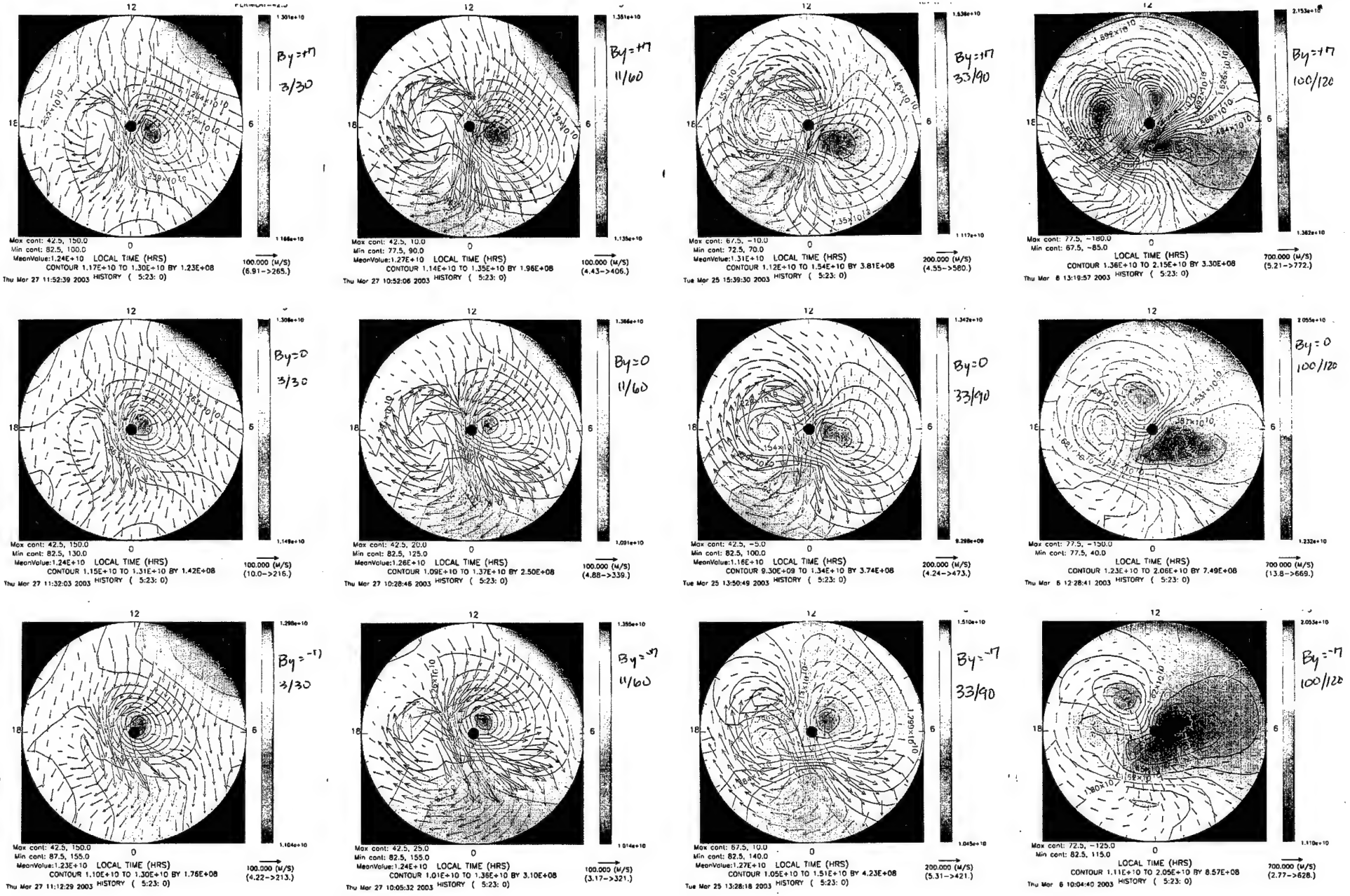

FIGURE 3

N2 140km 23 UT

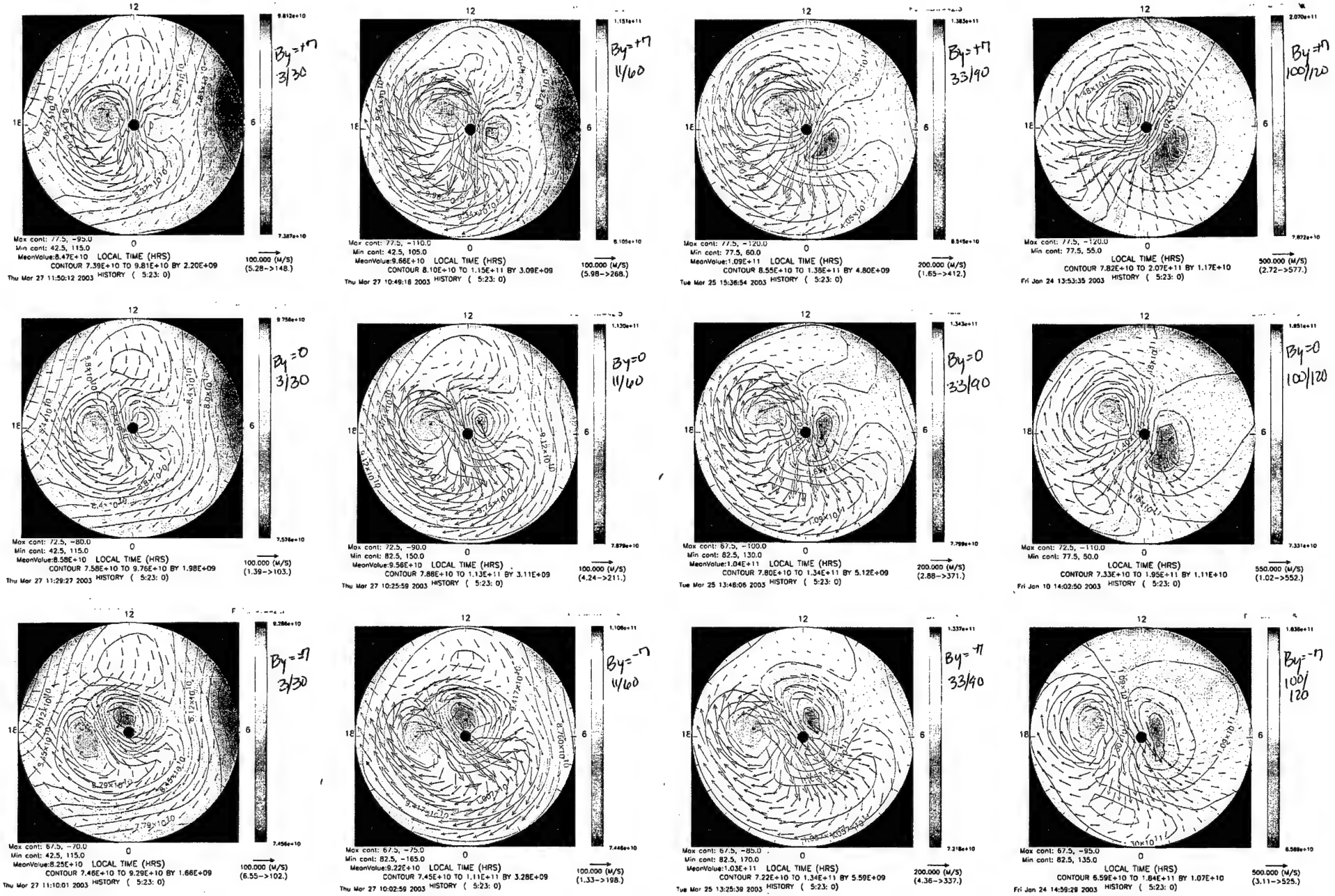

FIGURE 4

N2 200km 23UT

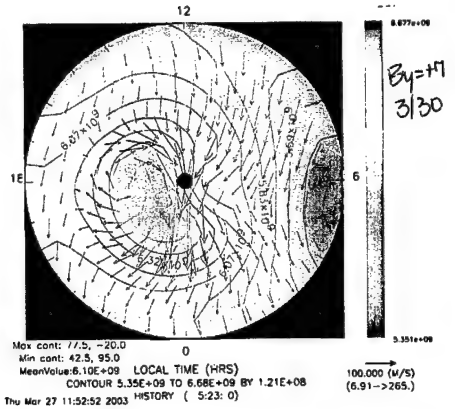

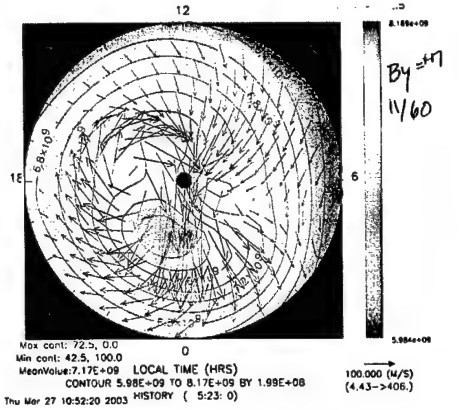

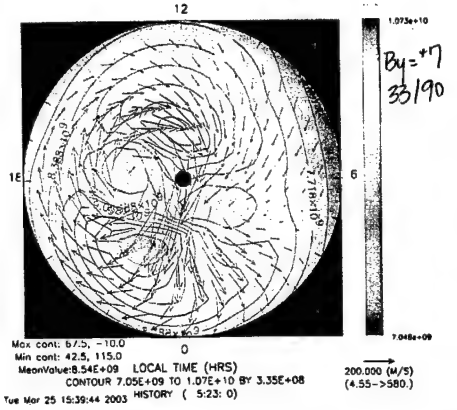

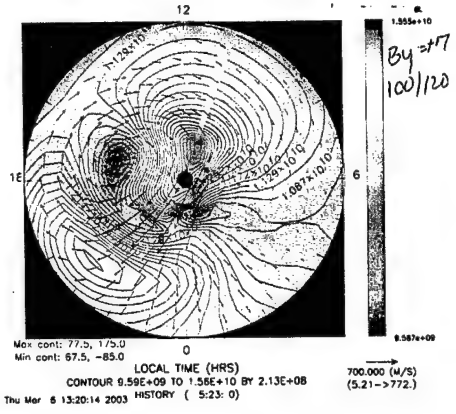

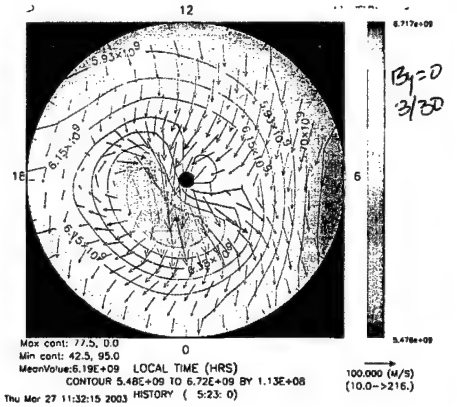

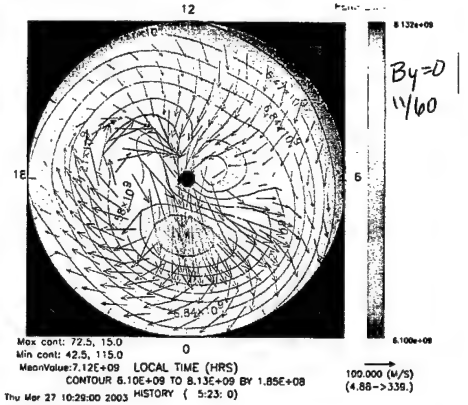

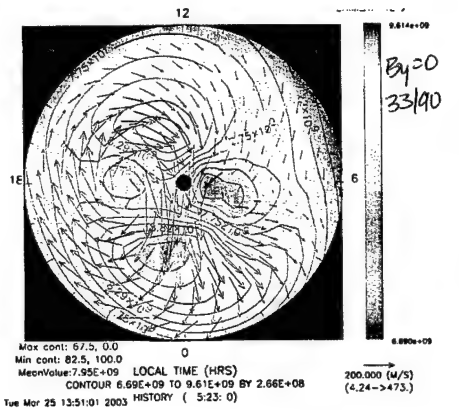

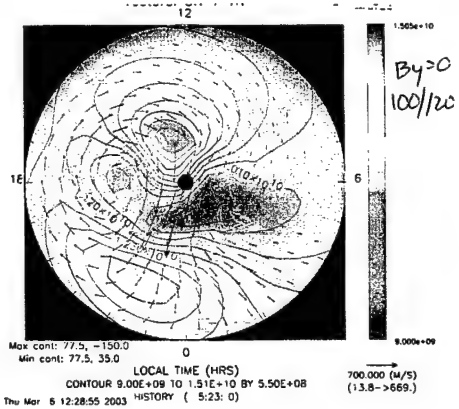

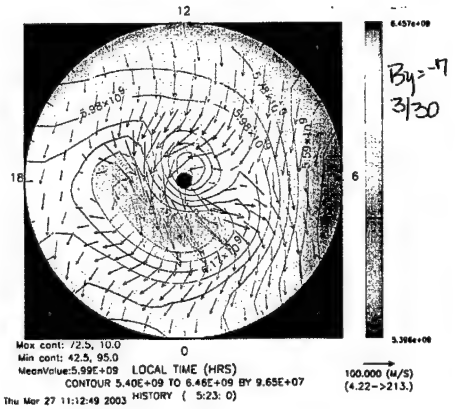

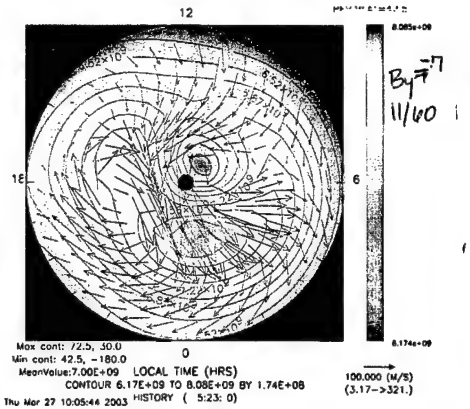

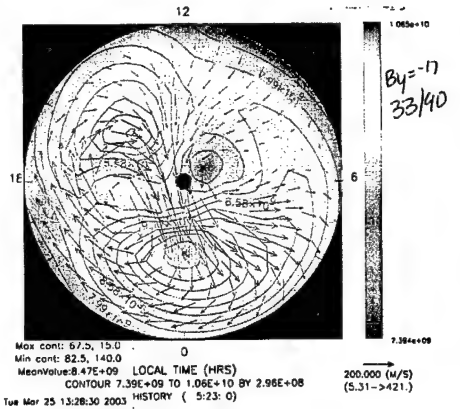

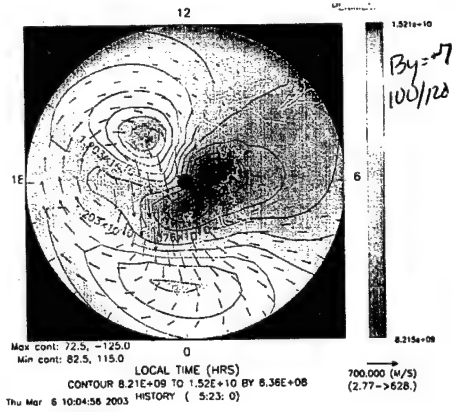

FIGURE 5

01 140km 23UT

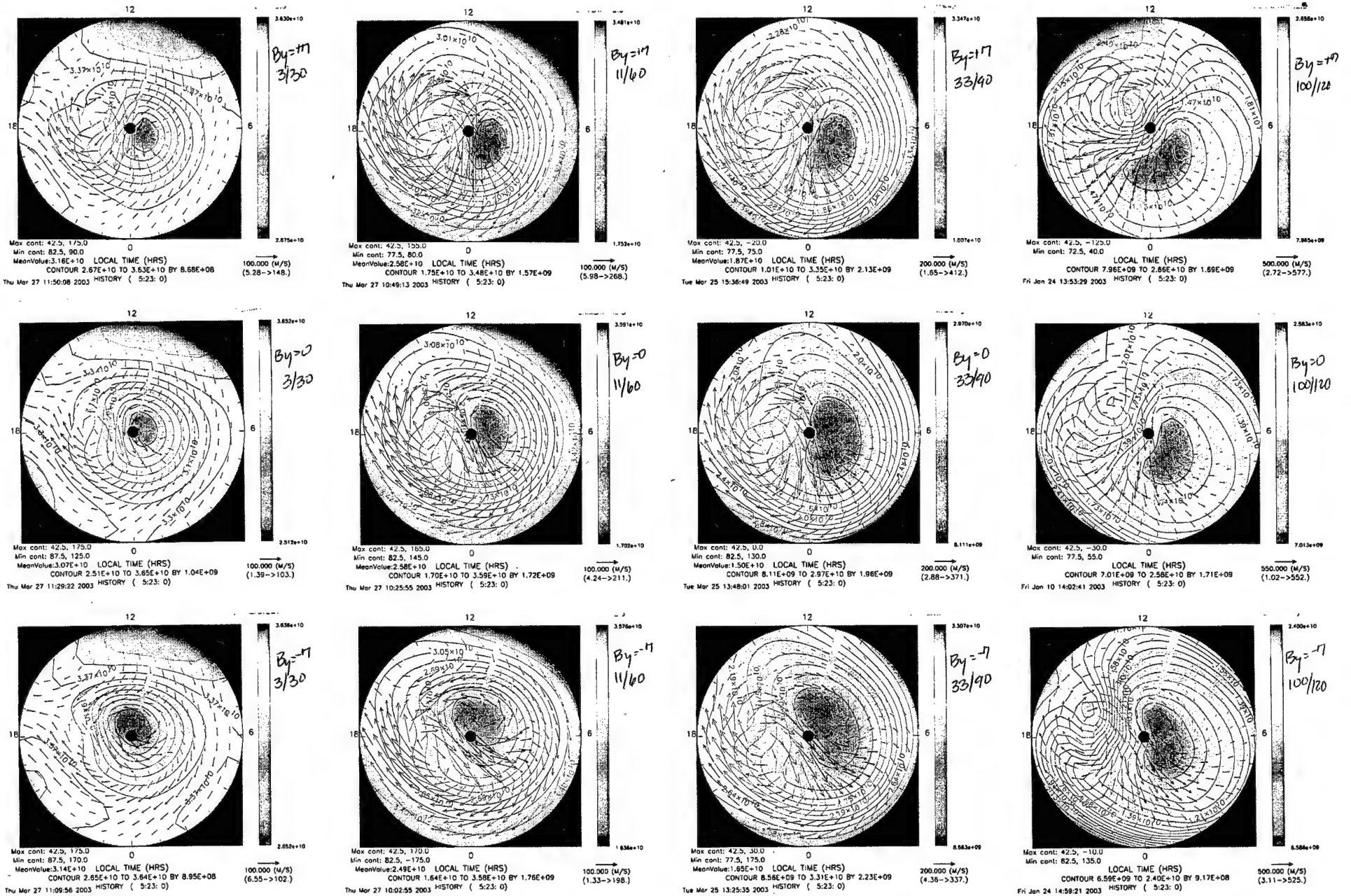

FIGURE 6

01 200km 23UT

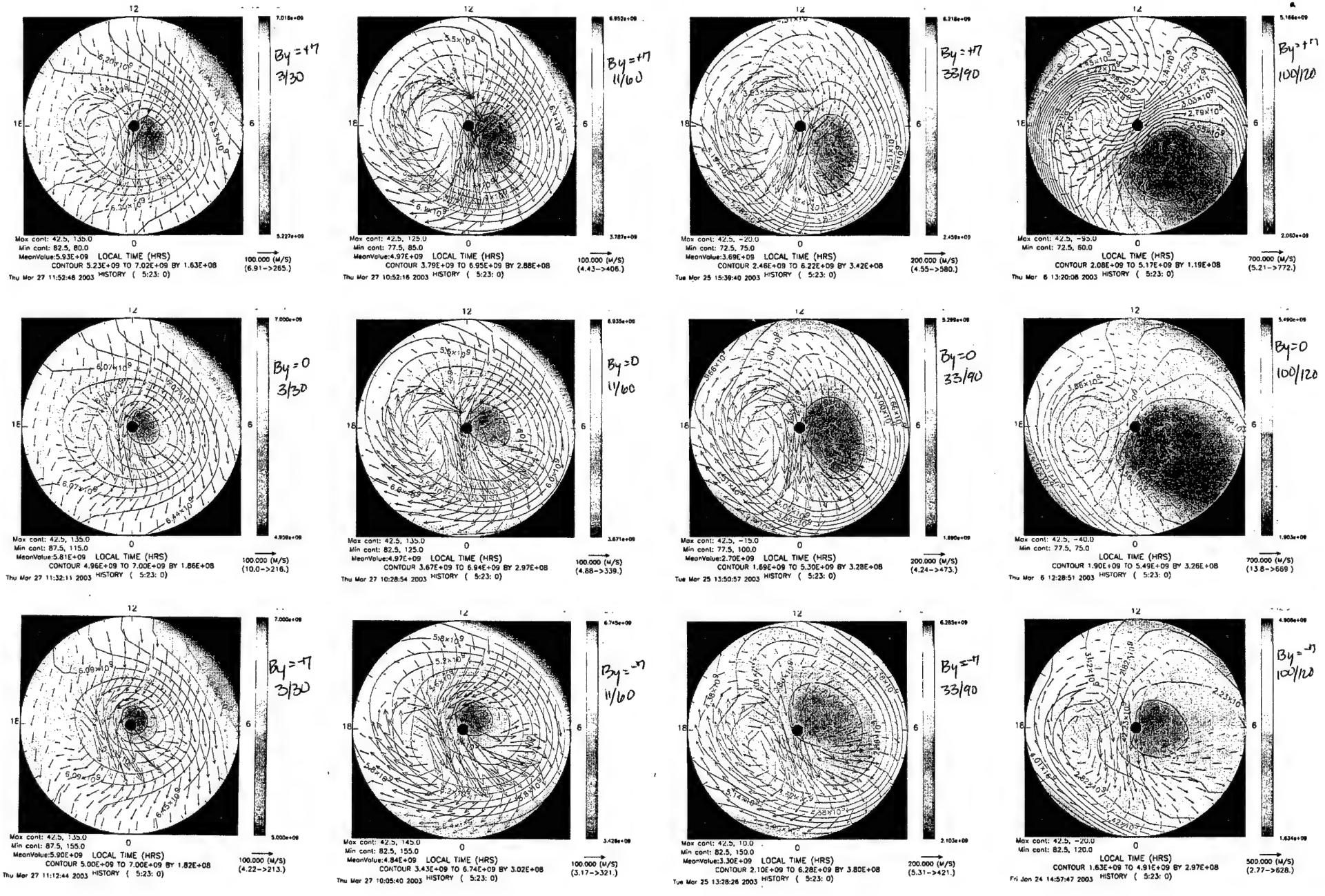

FIGURE 7

COL O/N2 200km 23UT

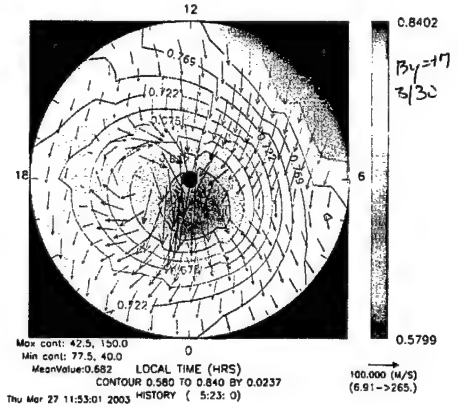

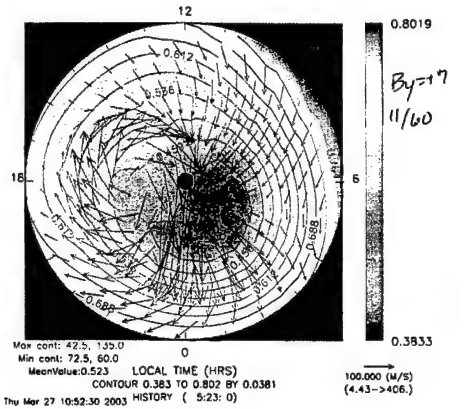

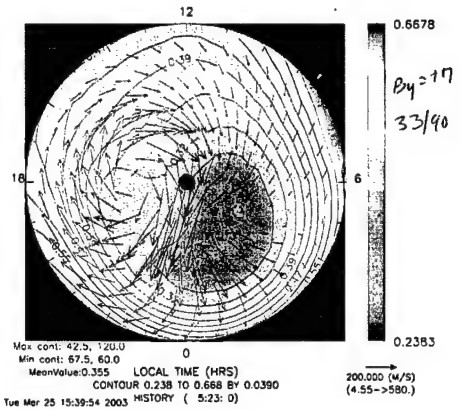

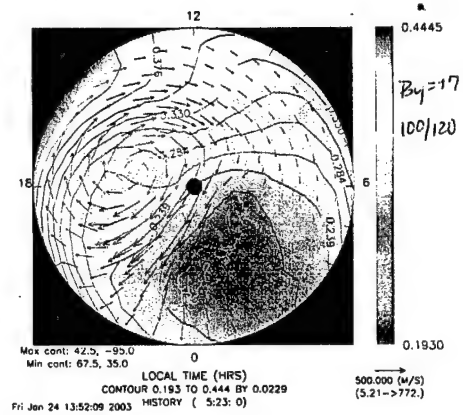

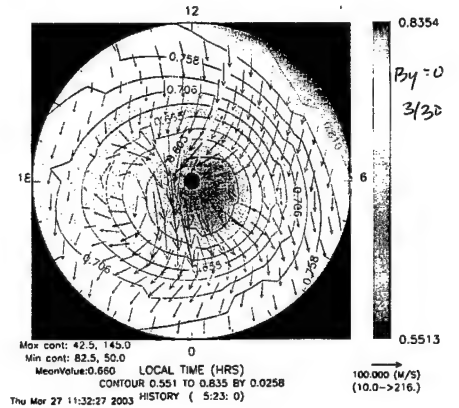

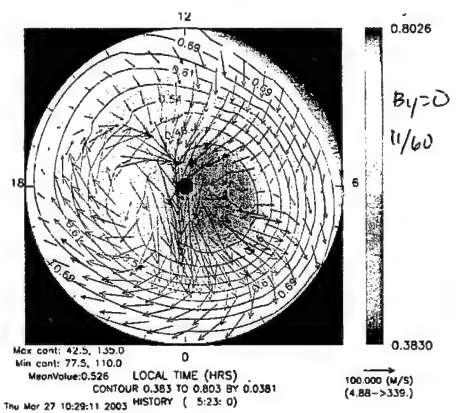

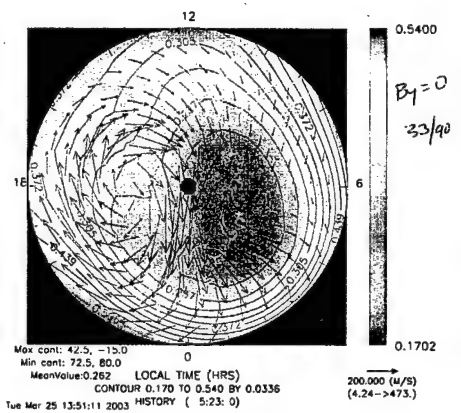

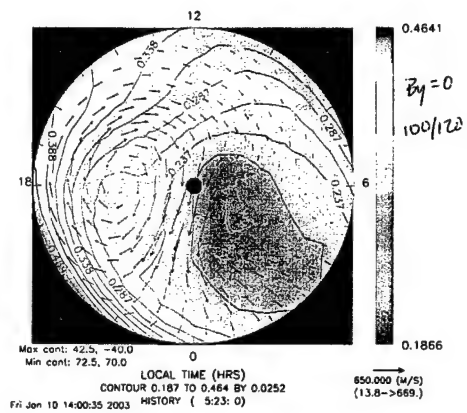

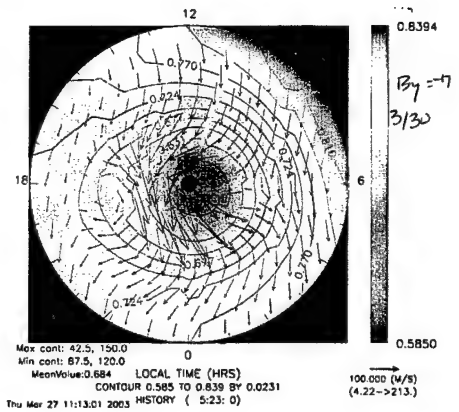

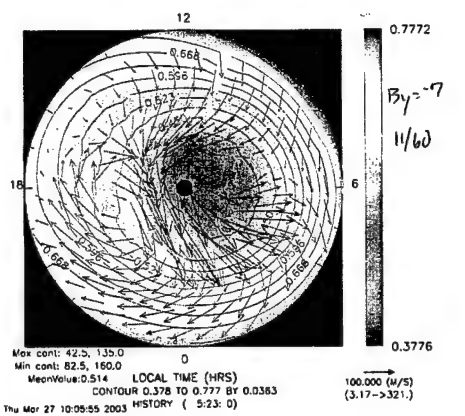

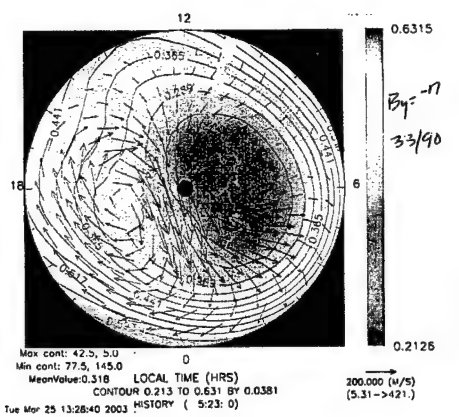

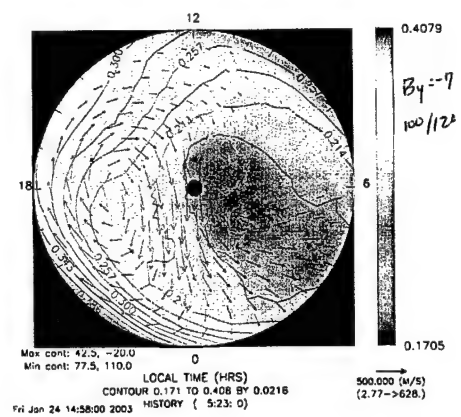

FIGURE 8

O/N2 140km 234T

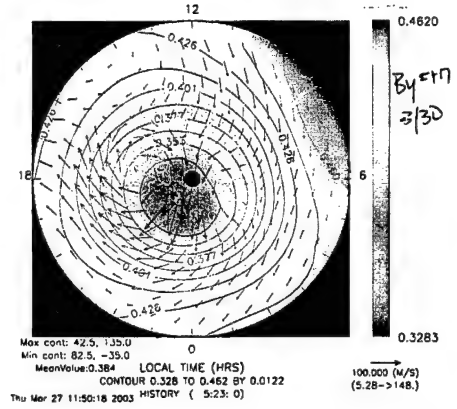

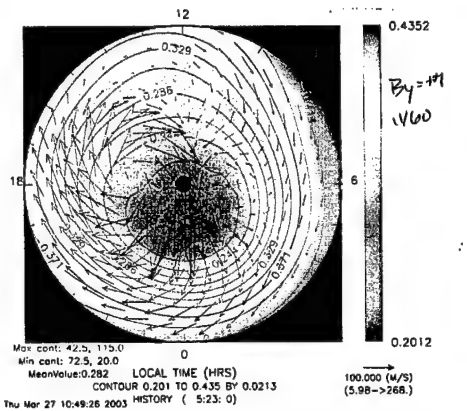

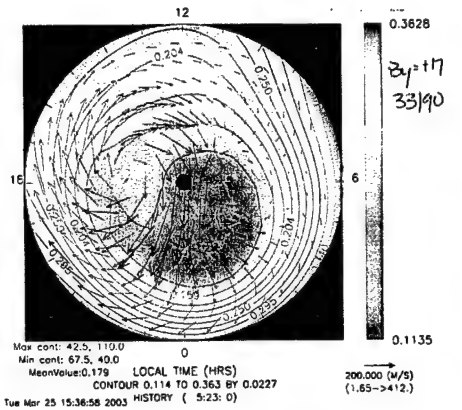

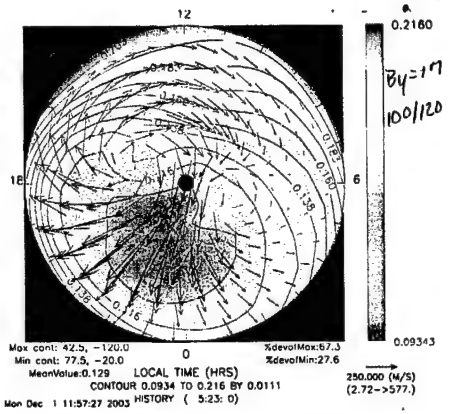

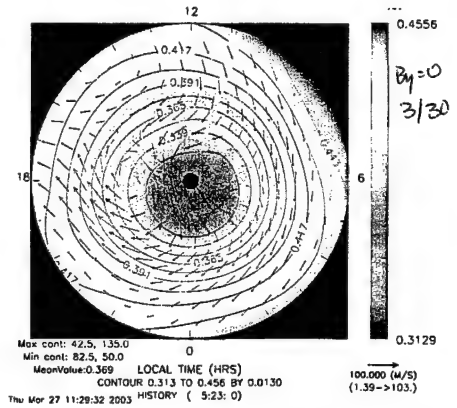

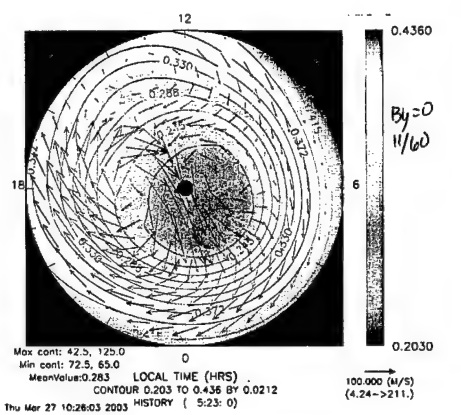

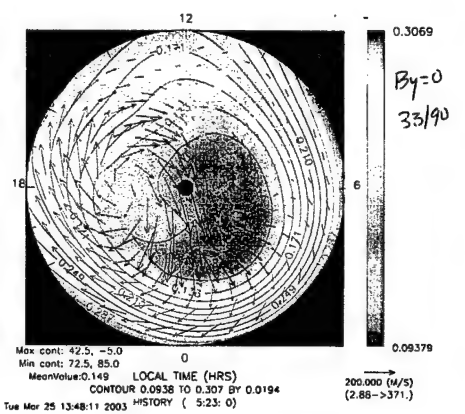

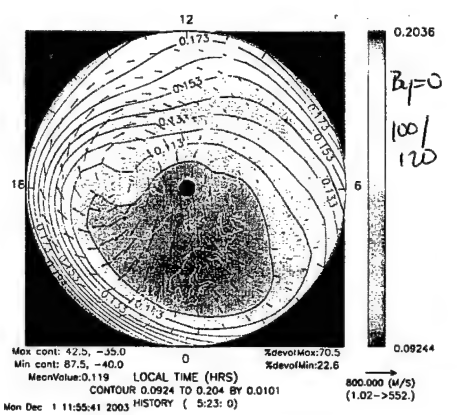

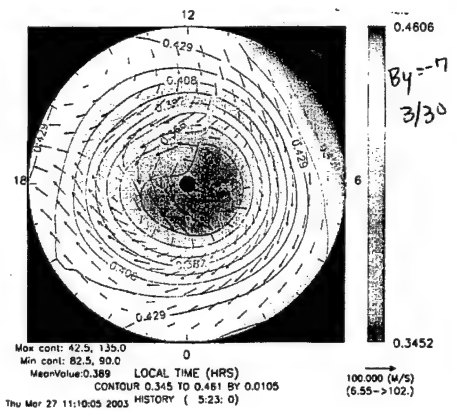

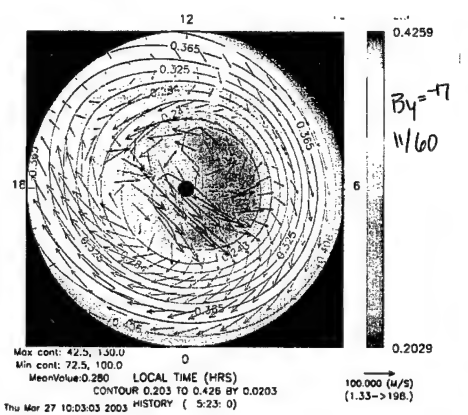

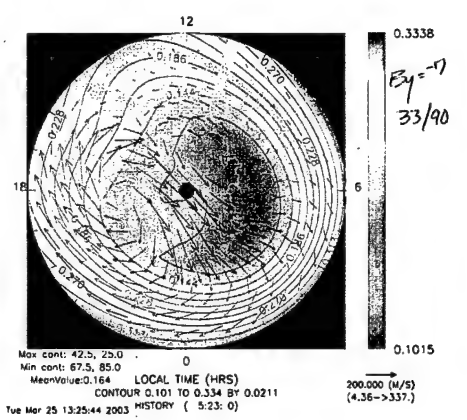

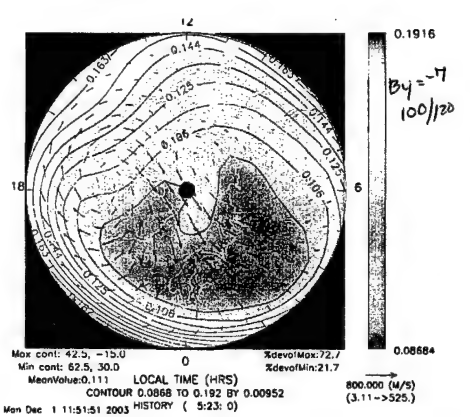

FIGURE 9

O/N2 200km 23UT

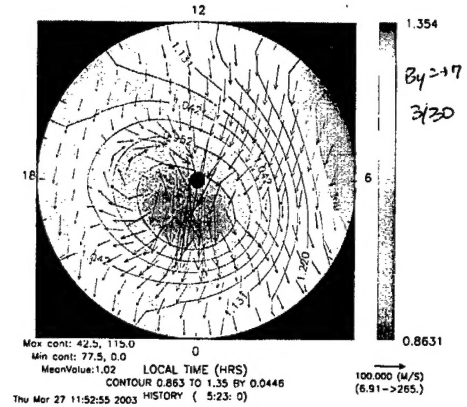

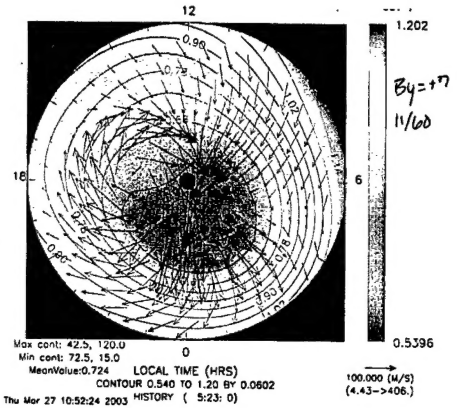

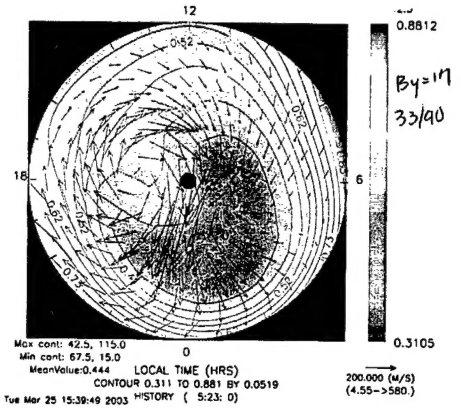

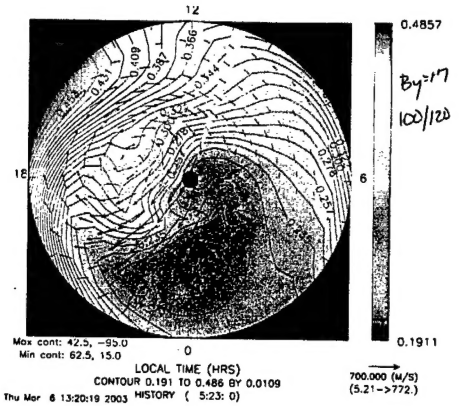

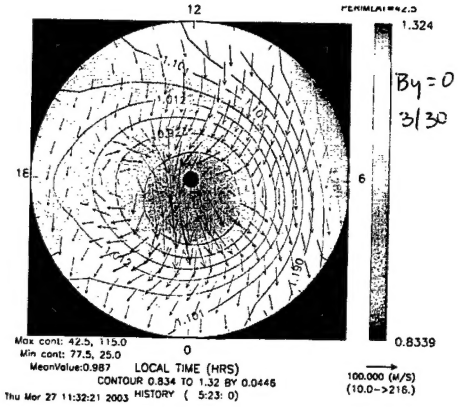

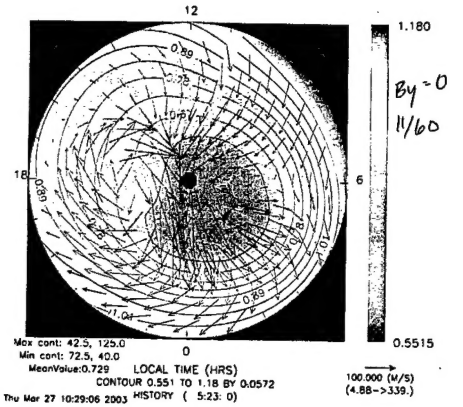

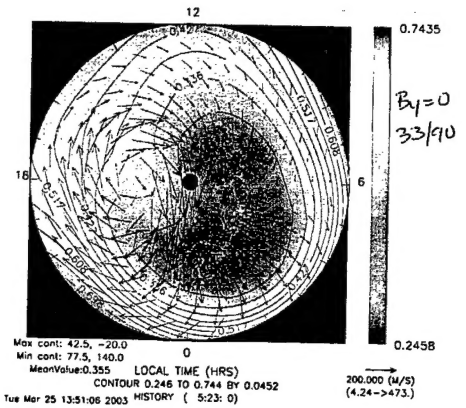

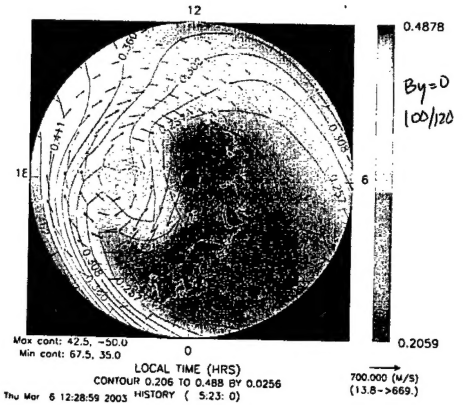

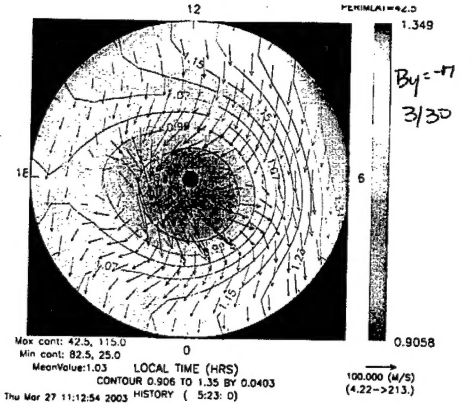

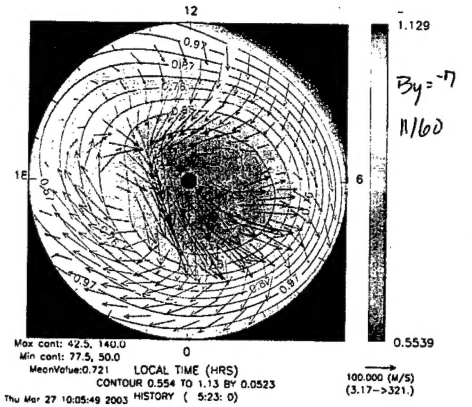

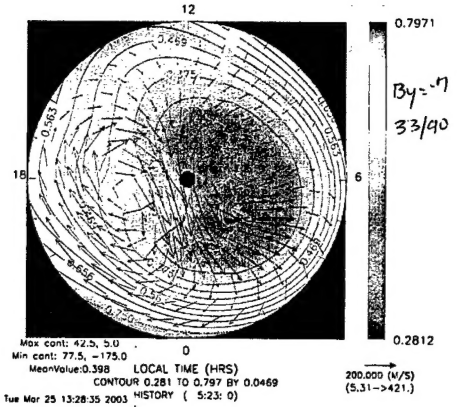

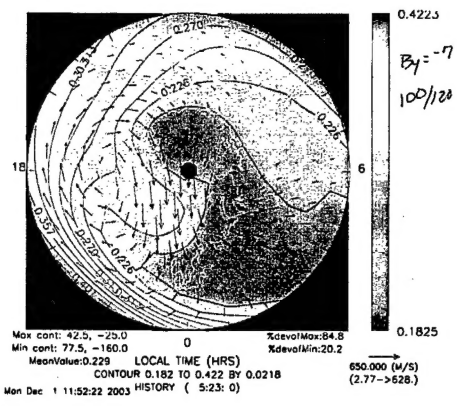

FIGURE 10

FIGURE 11 Coordinates of Minimum Densities as a Function of UT

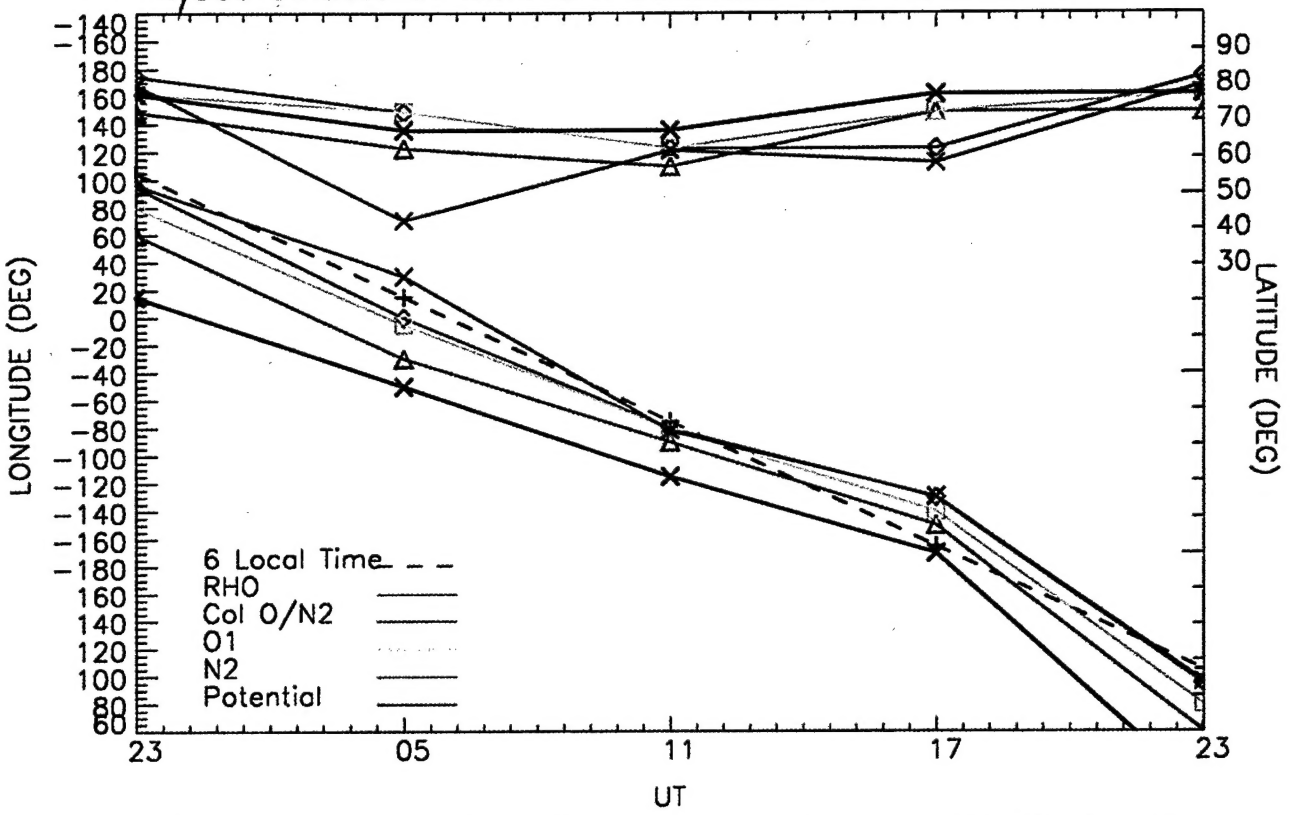

F10.7= 250 POWER= 11 CT_POTEN= 60 BY= 7 HEIGHT(km)= 140

Created on Thu Feb 20 09:56:35 2003
from: /home/steve/densityplot/data/mar_250_11_60_+7_NORTH_140km.txt

FIGURE 11

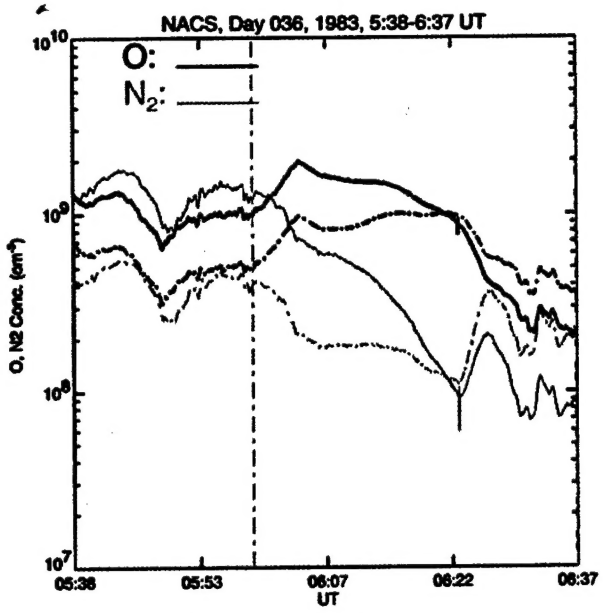

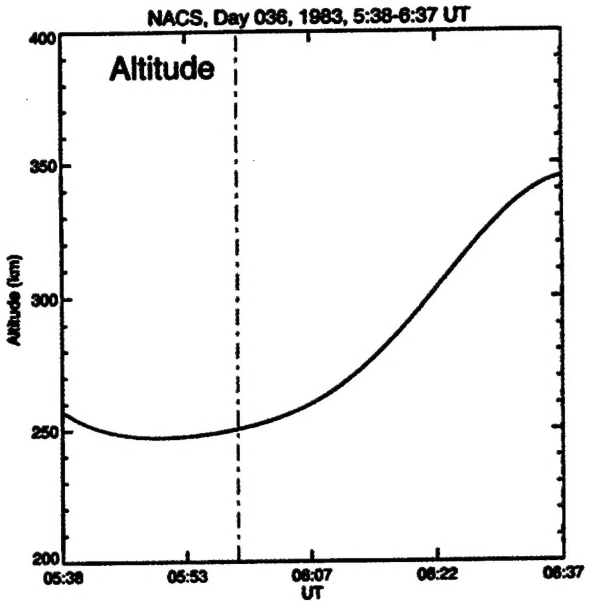

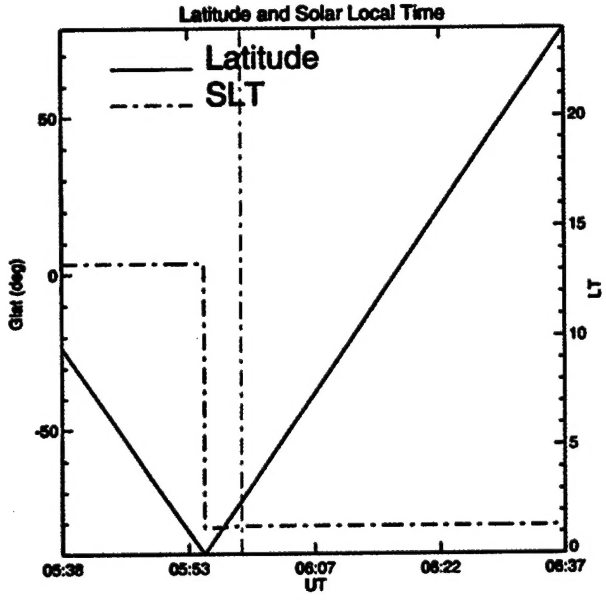

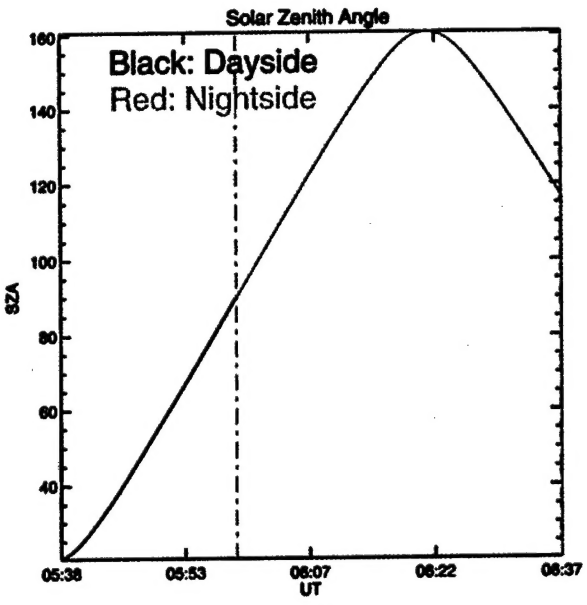

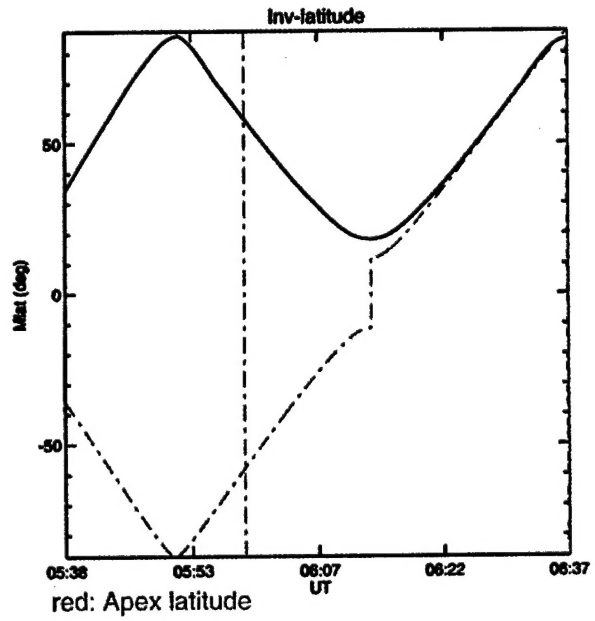

red: Apex latitude

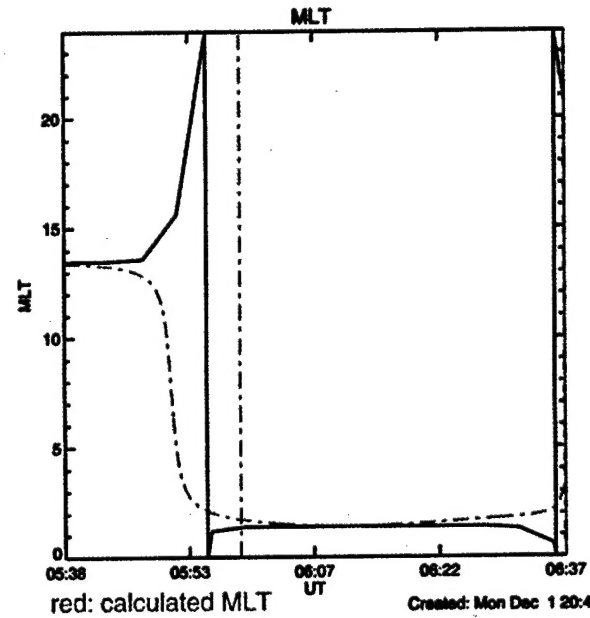

red: calculated MLT

Created: Mon Dec 1 20:45:36 2003

data/19830361053820_0_DE2_NACS_1S_V01.ASC

FIGURE 12

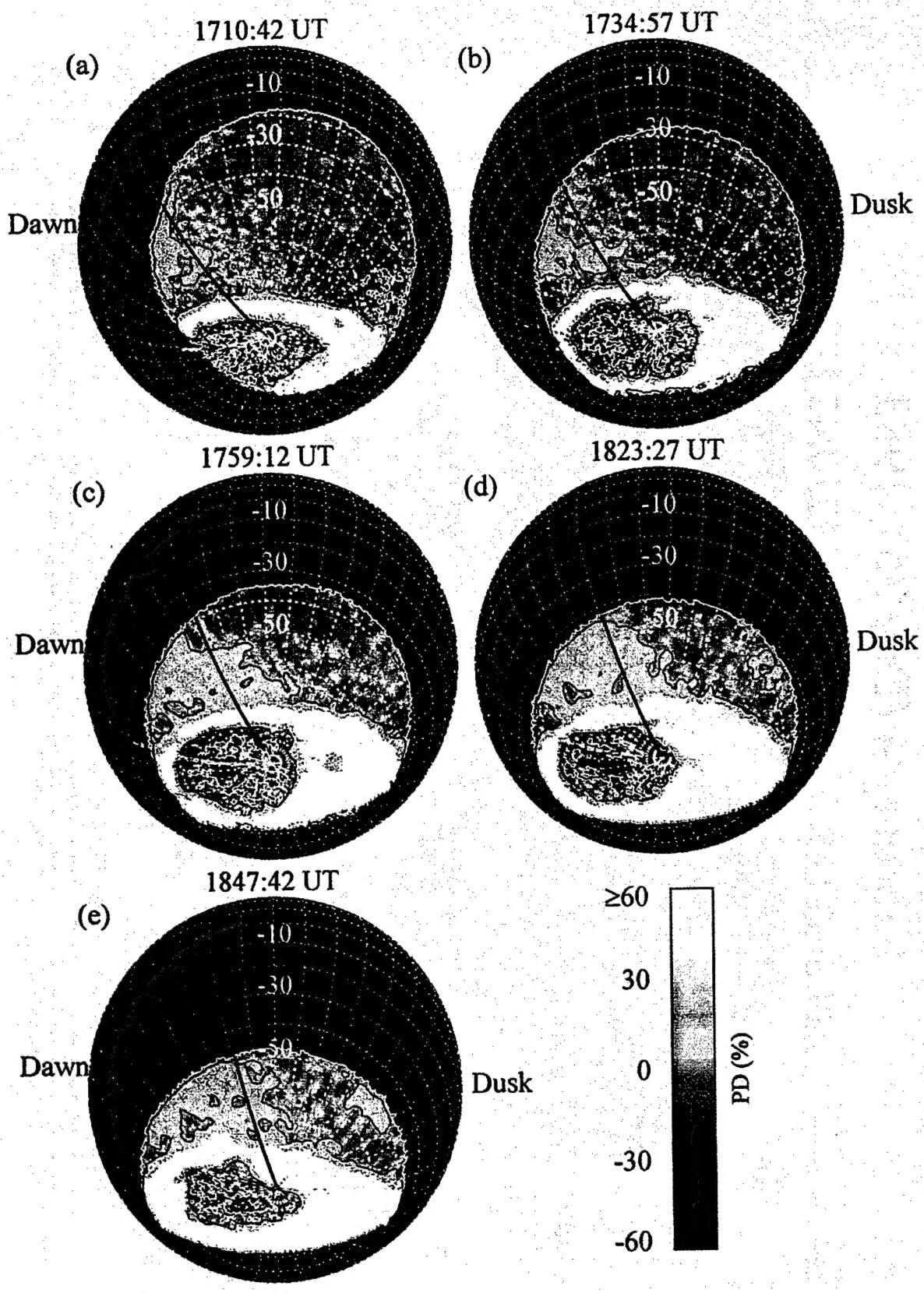

Plate 2. PD values for storm onset. Plotted PD values are from images smoothed with a 3x3 pixel moving filter. The dark line indicates 120°W geographic longitude, the meridian selected for particular study in later discussion. The noon-midnight meridian bisects each image vertically, with the morning sector to the left.

FIGURE 13